Journal of Medicinal Chemistry

Article

pubs.acs.org/jmc

Discovery of Small Molecules Targeting the Synergy of Cardiac Transcription Factors GATA4 and NKX2-5

Mika J. Välimäki,[†,‡,∥] Marja A. Tölli,[‡,∥] Sini M. Kinnunen,[†,‡] Jani Aro,[‡] Raisa Serpi,[‡] Lotta Pohjolainen,[†] Virpi Talman,[†] Antti Poso,[§] and Heikki J. Ruskoaho*[,†,‡]

[†]Division of Pharmacology and Pharmacotherapy, Faculty of Pharmacy, University of Helsinki, Helsinki FI-00014, Finland

[‡]Research Unit of Biomedicine, Department of Pharmacology and Toxicology, University of Oulu, Oulu FI-90014, Finland

[§]Faculty of Health Sciences, School of Pharmacy, University of Eastern Finland, Kuopio FI-70211, Finland

Supporting Information

ABSTRACT: Transcription factors are pivotal regulators of gene transcription, and many diseases are associated with the deregulation of transcriptional networks. In the heart, the transcription factors GATA4 and NKX2-5 are required for cardiogenesis. GATA4 and NKX2-5 interact physically, and the activation of GATA4, in cooperation with NKX2-5, is essential for stretch-induced cardiomyocyte hypertrophy. Here, we report the identification of four small molecule families that either inhibit or enhance the GATA4−NKX2-5 transcriptional synergy. A fragment-based screening, reporter gene assay, and pharmacophore search were utilized for the small molecule screening, identification, and optimization. The compounds modulated the hypertrophic agonist-induced cardiac gene expression. The most potent hit compound, *N*-[4-(diethylamino)phenyl]-5-methyl-3-phenylisoxazole-4-carboxamide (**3**, IC_{50} = 3 μM), exhibited no activity on the protein kinases involved in the regulation of GATA4 phosphorylation. The identified and chemically and biologically characterized active compound, and its derivatives may provide a novel class of small molecules for modulating heart regeneration.

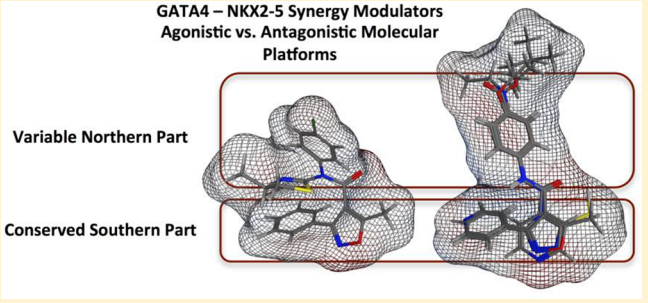

INTRODUCTION

The regulation of gene expression depends on specific *cis*-regulatory sequences that are located in gene promoter regions. These DNA sequences are recognized by tissue-specific transcription factors (TFs) in a sequence-specific manner, and their combinatorial interactions underlie physiological responses to developmental programs.[1−3] In the heart, developmental processes are controlled by an interplay among the master cardiac TFs, such as GATA4, NKX2-5, and TBX5.[4−6] These TFs bind to the promoters/enhancers of downstream targets as homo- or heteromultimeric complexes to physically interact with and synergistically regulate their target genes. GATA4 is one of the earliest-expressed TFs during cardiac development, and its up-regulation is sufficient to induce cardiogenesis in embryonic stem cells and promote a cardiac cell fate in noncardiogenic cells.[7] In the adult heart, GATA4 is a critical regulator of cardiac regeneration[8] and acts as a key transcriptional controller of numerous cardiac genes, including those encoding atrial natriuretic peptide (ANP),[9] B-type natriuretic peptide (BNP),[10] α-myosin heavy chain (α-MHC),[11] and β-MHC.[12] GATA4 binds to specific DNA response elements with or without cofactors, e.g., NKX2-5, TBX5, myocyte-specific enhancer factor 2 (MEF2), and serum response factor (SRF).[13] Mutational studies have shown that the GATA consensus sites in combination with an NKX2-5 binding element are important for the mechanical stretch-activated BNP transcription and sarcomere reorganization,[14] thus implicating the GATA4−NKX2-5 interaction for the response of cardiomyocytes to external stimuli, such as a hemodynamic overload due to high blood pressure and myocardial infarction.

GATA4 belongs to the GATA protein family (GATA1−6) and is characterized by *WGATAR*-recognizing zinc-finger domains that mediate DNA binding and protein−protein interactions. Our previous work illustrated that the protein assembly between GATA4 and NKX2-5, which is a critical GATA4 cofactor, imposes a structural fold that is similar to that of the evolutionally conserved DNA binding domains of nuclear receptors.[15] The significance of this particular protein−protein complex has been further validated by the co-occurrence of GATA4 and NKX2-5 in the binding site locations.[16] In addition to protein−protein interactions, the function of GATA4 is modulated through post-translational modifications. An increased GATA4 transcriptional activity has been shown in luciferase reporter assays with phosphorylated,[17] acetylated,[18] or sumoylated GATA4 protein.[19] Therefore, the functional modulation of the GATA4 protein or the GATA4−

Received: June 4, 2017
Published: August 31, 2017

DOI: 10.1021/acs.jmedchem.7b00816
J. Med. Chem. 2017, 60, 7781−7798

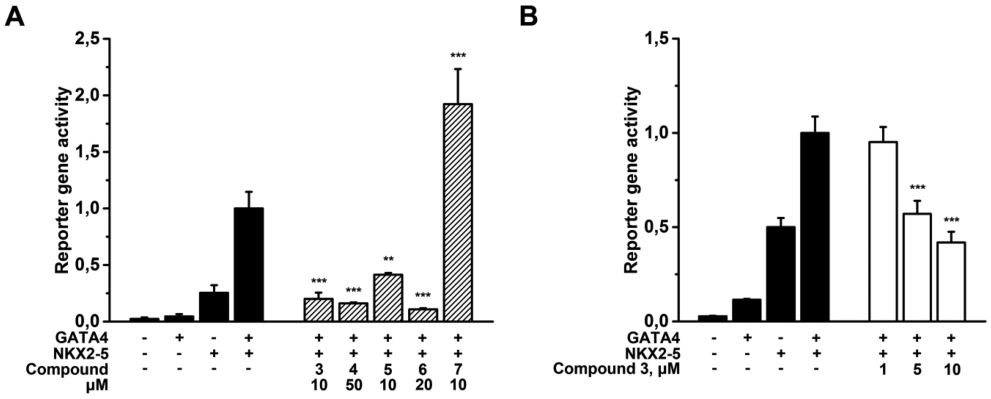

Figure 1. Cell-based reporter gene assay used for the screening of compound libraries targeting the GATA4−NKX2-5 transcriptional synergy. COS-1 cells were transfected with the 3xNKE-luciferase reporter construct and GATA4 and NKX2-5 expression plasmids and treated with small molecules for 24 h. The cells were lysed, and the luciferase reporter gene activity was measured by a luminometer. (A) Compounds **3**−**6** had a significant inhibitory effect on the GATA4−NKX2-5 transcriptional synergy, while compound **7** enhanced the GATA4−NKX2-5 transcriptional synergy. (B) Compound **3** dose-dependently inhibited the GATA4−NKX2-5 transcriptional synergy in the COS-1 cells. The data are shown as the mean ± SD, n = 2−9: (**) $p < 0.01$, (***) $p < 0.001$ vs vehicle treatment.

Scheme 1. Overall Flowchart Illustrating the Process of Screening and Validating the GATA4−NKX2-5 Synergy Modulators[a]

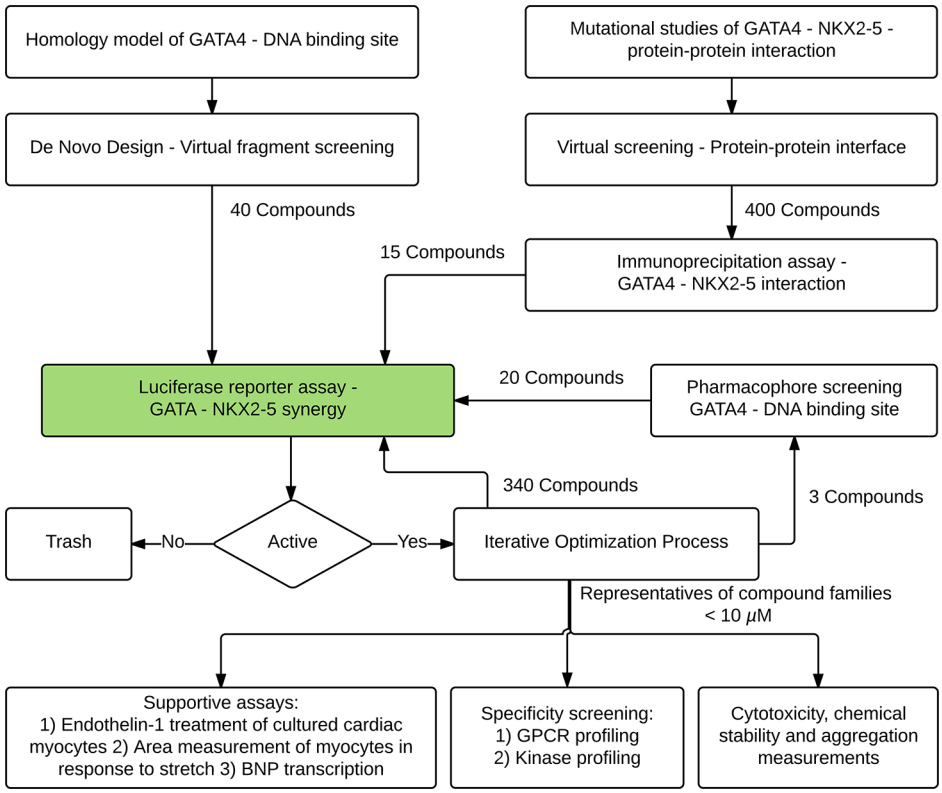

[a]BNP, B-type natriuretic peptide; GPCR, G-protein-coupled receptor.

NKX2-5 interaction could represent an innovative therapeutic approach for cardiac regeneration[20,21] or other pathophysiological conditions.[22] However, currently, there are no small molecule inhibitors or activators of GATA4 function except for one report describing inhibitors of GATA4 binding to DNA.[23] Here, we utilized a fragment-based screening, reporter gene assay based optimization, and pharmacophore search to identify small molecules that modify the synergy between the transcription factors GATA4 and NKX2-5 in vitro.

RESULTS

Primary Screening. Previously, we conducted a mutagenic analysis of the second zinc finger domain to elucidate the structural basis of the GATA4−NKX2-5 interaction.[15] These studies identified five highly conserved amino acids in the second zinc finger (N272, R283, Q274, K299) and its C-terminal extension (R319) that are critical for the physical and functional interaction with the third α helix of the NKX2-5 homeodomain. An integration of the experimental data with computational modeling suggested that the topology of the GATA4−NKX2-5 interaction resembles that of nuclear

DOI: 10.1021/acs.jmedchem.7b00816
J. Med. Chem. 2017, 60, 7781−7798

Scheme 2. Chronological Workflow of the Hit Compound Search and Optimization Process Initiated from the Active Fragments[a]

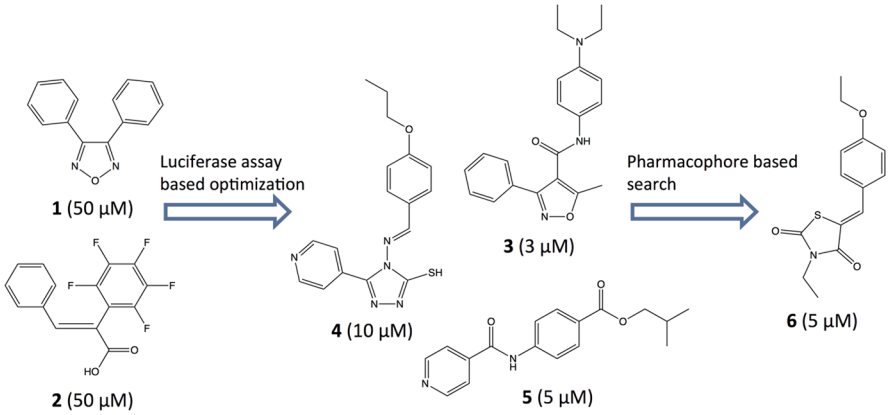

[a]Scheme illustrates the molecular structure, compound code numbers, and corresponding IC_{50} values in the GATA4−NKX2-5 luciferase reporter gene assay.

Table 1. Structural Variants of Hit Compound 3 in the Luciferase Reporter Gene Assay[28]

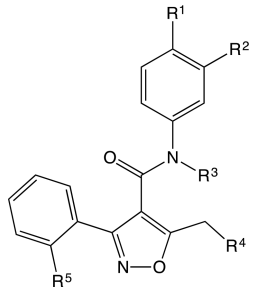

Compound	R^1	R^2	R^3	R^4	R^5	IC_{50}/K_a[a] (μM)
3	-N(CH_2CH_3)$_2$	-H	-H	-H	-H	3
7	-Cl	-H		-H	-H	7[a]
8	-OCF_3	-H	-H	-H	-H	11
9	-OCH(CH_3)$_2$	-H	-H	-H	-H	13
10	-CN	-Cl	-H	-H	-H	16
11	-CH(CH_3)$_2$	-H	-H	-H	-H	16
12			-H	-H	-H	17
13	-C(CH_3)$_3$	-H	-H	-H	-H	18
14	-OCH_2CH_3	-H	-H	-H	-H	20
15	-CO_2CH(CH_3)$_2$	-H	-H	-H	-H	20
16	-H		-H	-H	-H	20
17		-H	-H	-H	-H	20
18	-H		-H	-H	-H	20
19	-CH(CH_3)(CH_2CH_3)	-H	-H	-H	-Cl	20
20	-C(CH_3)$_3$	-H	-H	-H	-Cl	22
21			-H	-H	-H	23
22		-H	-H	-H	-H	28
23	-H		-H	-H	-H	28

Compound	R^1	R^2	R^3	R^4	R^5	IC_{50}/K_a[a] (μM)
24	-CH(CH_3)(CH_2CH_3)	-H	-H	-H	-H	32
25	-H		-H	-H	-H	33
26		-H	-H	-H	-Cl	38
27	-OC_6H_5	-H	-H	-H	-H	>50
28		-H	-H	-H	-H	>50
29	-$OCH_2CH_2CH_3$	-H	-H	-H	-H	>50
30	-$CO_2CH_2CH_2CH_3$	-H	-H	-H	-H	>50
31	-$NHCH_2CH_3$	-H	-H	-H	-H	>50
32	-$NHCH_2CH_3$	-H	-H	-OH	-H	>50
33	-CH_3	-SO_2N(CH_2CH_3)$_2$	-H	-H	-H	>50
34	-H	-SO_2N(CH_2CH_3)$_2$	-H	-H	-H	>50
35		-H	-H	-H	-H	>50
36		-H	-H	-H	-H	>50
37		-H	-H	-H	-H	>50
38		-H	-H	-H	-H	>50
39		-H	-H	-H	-H	>50

[a]K_a is equal to the synergy activation.

DOI: 10.1021/acs.jmedchem.7b00816
J. Med. Chem. 2017, 60, 7781−7798

receptors.[15] In agreement with those observations, GATA4 has a synergistic effect with NKX2-5 on promoters that contain multiple NKX2-5 high affinity response elements (NKEs).[24,25] To evaluate the effect of the compounds on the functional interaction between GATA4 and NKX2-5, we developed a luciferase reporter gene assay specifically for the GATA4−NKX2-5 transcriptional synergy.[15] In this assay, mammalian COS-1 cells were transfected with the protein expression vectors pMT2-GATA4, pMT2-NKX2-5, both pMT2-GATA4 and pMT2-NKX2-5, or the empty control vector pMT2. The transfection efficiencies of the vectors in the COS-1 cells were verified by defining the protein levels of GATA4 and NKX2-5 by Western blotting.[15] Typically, several limitations are associated with the use of luciferase reporter assays.[26] The tested compounds may interfere with the luciferases and decrease the assay signal, resulting in false positives. In addition, the compounds may aggregate, have redox behavior, enzymatically inhibit the reporter, or form complexes that interfere with the fluorescence. Therefore, the positive findings obtained here with the primary screening assay were further confirmed using bioassays. As shown in Figure 1, the NKX2-5 protein activates the construct containing three high affinity NKX2-5 binding sites alone and synergistically with GATA4, while the GATA4 protein alone had only a negligible effect.

Initially, the compounds selected by the virtual screening for the modulation of protein−protein interaction were tested using an immunoprecipitation screening method, which revealed 15 weak inhibitory compounds (Scheme 1). However, the identified compounds were shown to be false positives in the luciferase reporter assay and confirmatory bioassays, and subsequently, this approach was discontinued.

An in silico analysis focusing on the DNA binding site in the C-terminal zinc finger of GATA4 was carried out using a collection of 39 randomly placed molecular fragments, followed by energy minimization to reveal and rank the interaction potentials of the fragments inside the implied binding cavity. The compiled virtual assignments at the DNA binding site with multiple copies of simultaneous chemical probes[27] suggested a pronounced electrostatic interaction among the rigid fragment compounds with a negative charge/acceptor and aromatic features. On the basis of these theoretical annotations, a cherry-picked collection of 40 fragment compounds was purchased and tested in vitro using the GATA4−NKX2-5 luciferase reporter gene assay. These experiments identified two compounds that inhibited the transcriptional synergy, i.e., 3,4-diphenyl-1,2,5-oxadiazole (compound **1**) and 2-perfluorophenyl-3-phenylacrylic acid (compound **2**), at a concentration of 50 μM (Scheme 2).

Hit Optimization. A luciferase reporter gene assay based optimization of the initial fragment compounds was achieved by introducing sequential structural modifications and fragment growth to uncover compounds with activity on the GATA4−NKX2-5 transcriptional synergy. First, variable substituents were inserted into the three-ring core of fragment **1**. The compounds with the para-substituted six-member ring were the most effective. Second, different linkers with variable bond lengths and chemical compositions were inserted between the six- and five-member rings. The number of heavy atoms between the aromatic rings of the compounds ranged from zero to three. The most potent compound according to the luciferase reporter gene assay, at a concentration of 10 μM, was *N*-[4-(diethylamino)phenyl]-5-methyl-3-phenylisoxazole-4-carboxamide (**3**) (Figure 1A), which dose-dependently inhibited the GATA4−NKX2-5 transcriptional synergy (Figure 1B).[28] A relatively rigid two heavy atom linker and the hydrogen acceptor feature next to the five-member ring were the essential structural features in successful fragment-to-hit growth (Scheme 2). During the primary screening and hit optimization, 800 small molecule entities were tested, including at least 15 structurally related compounds in each of the three active series to confirm the original findings and the structure−activity relationships (Tables 1−3).

Pharmacophore Search. To further evaluate the active molecular scaffold space, a pharmacophore model was built based on the following three active compounds: **3**, 4-[(4-propoxybenzylidene)amino]-5-(pyridin-4-yl)-4*H*-1,2,4-triazole-3-thiol (**4**), and isobutyl 4-(isonicotinamido)benzoate (**5**) (Figure 2). All three active compounds have a relatively rigid core structure, and therefore, the low energy conformations of these compounds were used as a basis for the compound superimposition and pharmacophore model. Subsequently, the pharmacophore model was completed with excluding volumes derived from the homology model of the GATA4-DNA binding site. Furthermore, 15 inactive and structurally variable compounds were selected from the parallel screening path targeting the GATA4−NKX2-5 protein−protein interface. Here, 14 of the 15 compounds screened was not detected by the pharmacophore model. Finally, an in silico screening of the commercial compound library was carried out using the pharmacophore model. Consequently, 20 compounds were purchased and tested in vitro using the luciferase reporter gene assay, leading to the identification of a new active compound, 5-(4-ethoxybenzylidene)-3-ethylthiazolidine-2,4-dione (**6**) at a concentration of 5 μM, and its variants (Table 4).

All four compound families found during the in vitro screening inhibited the GATA4−NKX2-5-induced synergistic activation of the promoter containing the three high affinity NKX2-5 binding sites. Interestingly, the reporter assay screening also detected several weak hit compounds with the potential to increase the GATA4−NKX2-5 transcriptional synergy. These compounds have variable scaffolds but the structural elements were similar to the structures that inhibited the activation. Subsequently, during the small molecule optimization of the inhibitory compound **3**, surprisingly, we detected a compound that strongly augmented the GATA4−NKX2-5 synergy in the reporter gene assay (Figure 1A). The structure of this activator compound, *N*-(4-chlorophenyl)-5-methyl-*N*-(4-methyl-4,5-dihydrothiazol-2-yl)-3-phenylisoxazole-4-carboxamide (**7**), partially overlaps the pharmacophore model, which was developed based on inhibitory compounds with an additional five-member ring moiety attached. Due to the complexity of the compound structure, the synthesis of its derivatives was not pursued in this study, and only one related compound was tested to confirm this finding. Furthermore, the screening of a small natural compound library identified the flavonoids apigenin and luteolin as weak inhibitors of the GATA4−NKX2-5 transcriptional synergy with IC_{50} values of 24 and 22 μM, respectively.

Aggregation of the Compounds. Aggregation of a compound may result in artificial activity in luciferase enzyme based assays.[26] To evaluate the potential aggregation of the compounds **3**, **4**, and **7**, the testing conditions were mimicked, and the light scattering of any particles/aggregates in the mixture was measured using the nephelometric method. Aggregation was only observed in the samples at a concentration of 100 μM. At lower concentrations, the values

DOI: 10.1021/acs.jmedchem.7b00816
J. Med. Chem. 2017, 60, 7781−7798

Table 2. Structural Variants of Hit Compound 4 in the Luciferase Reporter Gene Assay

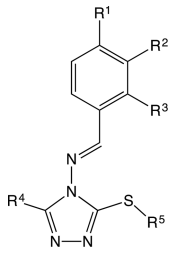

Compound	R^1	R^2	R^3	R^4	R^5	IC_{50} (μM)
4	-$OCH_2CH_2CH_3$	-H	-H		-H	10
40	-$N(CH_2CH_3)_2$	-H	-H		-H	6
41	-OCH_2CH_3	-H	-H		-H	7
42	-$N(CH_3)_2$	-H	-H		-H	7
43	-$C(CH_3)_3$	-H	-H		-H	7
44	-H	-OCH_3	-OCH_3		-H	8
45	-H	-H	-OCH_2CH_3		-H	8
46	-OCH_3		-H		-H	10
47	-OCH_3	-CH_3	-H		-H	11
48	-H		-H		-H	13
49	-$N(CH_2CH_3)_2$	-H	-H		-H	19
50	-H		-OH		-H	20
51	-OCH_3	-CH_3	-H		-CH_3	24
52	-$C(CH_3)_3$	-H	-H		-H	30
53	-OCH_2CH_3	-OCH_2CH_3	-H		-CH_3	30
54		-H	-H		-H	37
55	-$OCH_2CH_2CH_2CH_3$	-H	-H	-CH_2CH_3	-H	>50
56	-$CH(CH_3)_2$	-H	-H		-H	>50
57	-H	-OCH_3	-OCH_3		-CH_3	>50
58	-$N(CH_2CH_3)_2$	-H	-OCH_3		-H	>50
59	-H	-F	-H		-H	>50
60	-H	-OCH_3	-H		-H	>50
61	-H	-CH_3	-H		-H	>50

Table 3. Structural Variants of Hit Compound 5 in the Luciferase Reporter Gene Assay

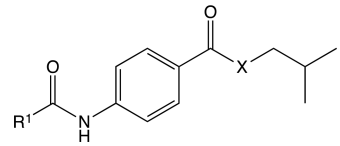

Compound	R^1	X	IC_{50} (μM)
5		O	5
62		O	9
63		N	23
64	-CH_2CH_2COOH	O	37
65	-CF_3	N	42
66		N	>50
67		N	>50
68		O	>50
69		N	>50
70		N	>50
71		O	>50
72		N	>50
73	-$CH_2CH_2CH_3$	N	>50
74	-$CH(CH_2CH_3)_2$	N	>50

were close to those observed in the blanks, indicating that there is no detectable aggregation, except for compound **7**, which shows minor signs of aggregation at 30 μM (Figure S1 in Supporting Information).

Chemical Stability of Compound 3. In addition, the stability of compound **3** was studied for 5 and 10 days in mouse embryonic stem cells (mESCs) in vitro at two different concentrations (3 and 5 μM) with two blank treatments (DMSO and embryoid body differentiation medium (EBDM)) added to the cell culture media. The intra- and extracellular concentrations of compound **3** and metabolite **31** were measured by HPLC/MS after performing specific sample pretreatment and extraction procedures. The results demonstrate that compound **3** is only modestly degraded during the 10 days in the cellular assay (Table S1). Furthermore, the storage of compound **3** in DMSO at room temperature for 6 months did not result in degradation (data not shown).

DOI: 10.1021/acs.jmedchem.7b00816
J. Med. Chem. 2017, 60, 7781−7798

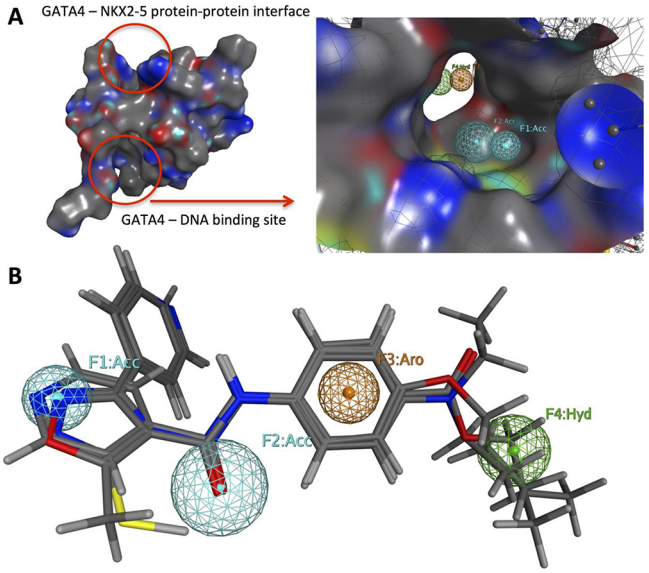

Figure 2. (A) C-terminal zinc finger of GATA4 mediates the DNA binding and GATA4–NKX2-5 protein–protein interaction. Computational methods were applied to analyze and screen two separate binding sites. A pharmacophore model with excluded volumes was built for the DNA binding cavity of GATA4. (B) The low energy conformations of compounds **3**, **4**, and **5** were utilized as a basis for the pharmacophore model. All three compounds inhibited the GATA4–NKX2-5 synergy in the luciferase reporter gene assay. Atom colors are the following: white = hydrogen, gray = carbon, red = oxygen, blue = nitrogen, and yellow = sulfur. Pharmacophore features are the following: blue sphere = acceptor, orange sphere = aromatic, and green sphere = hydrophobic.

Table 4. Structural Variants of Hit Compound 6 in the Luciferase Reporter Gene Assay

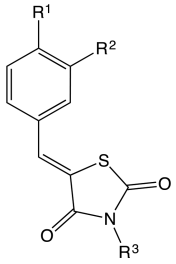

Compound	R^1	R^2	R^3	IC_{50} (μM)
6	$-OCH_2CH_3$	-H	$-CH_2CH_3$	5
75		-F	$-CH_2CH_3$	8
76	$-N(CH_3)_2$	-H	$-CH_2CH_2CH(CH_3)_2$	10
77	-H	$-NO_2$	-H	20
78	$-CH_2CH_3$	-H	-H	21
79	$-OCH_2CH_3$	$-OCH_2CH_3$	$-CH_2CH_3$	26

GATA4 Transcriptional Activity and GATA4–NKX2-5 Interaction. Compounds **3**, **4**, and **7** were evaluated in a reporter assay in COS-1 cells by using BNP promoter reporter constructs containing either the first 60 bp in the BNP promoter including the proximal TATA-box (BNP minimal promoter) (Figure S2A) or the first 90 bp that include also the tandem GATA-site (Figure S2B). TATA-box in BNP promoter acts as a functional GATA4 binding site.[13] Compound **3** significantly inhibited GATA4 driven transactivation of luciferase reporter constructs containing either BNP minimal promoter (Figure S2A) or BNP promoter containing minimal promoter and tandem GATA-site on −90 bp (Figure S2B). Compound **4** showed similar tendency, yet a statistically significant inhibition of gene transactivation was seen only with construct containing both minimal promoter and tandem GATA-sites (Figure S2B). Overall, the effects of all compounds parallel those of primary screening assay with promoter containing the three high affinity NKX2-5 binding sites and are in agreement with the compound's hypothetical mechanism of action. In addition, we used an immunoprecipitation assay to characterize further GATA4–NKX2-5 interaction. GATA4 and NKX2-5 FLAG protein lysates were produced in COS-1 cells, and FLAG-antibody bind agarose beads were used to pull down NKX2-5 together with interacting GATA4. As shown in Figure S3, compound **3** modestly decreased the intensity of GATA4–NKX2-5 interaction, although this change was not statistically significant (Figure S3).

GATA4 and NKX2-5 DNA Binding. Previously, El-Hachem and Nemer have identified molecules that prevent GATA4 activity by inhibiting its interaction with DNA and blocking the activation of the downstream target genes of GATA4.[23] These effects were reported to be due to a decreased GATA4-DNA interaction as evaluated by an electrophoretic mobility shift assay (EMSA). To determine whether the active compounds identified in the present study influence GATA4 or NKX2-5 DNA binding, we performed EMSA using nuclear proteins from both COS-1 cells and neonatal rat cardiomyocytes. The compounds were incubated with the COS-1 nuclear proteins, and then a ^{32}P-labeled oligonucleotide targeting GATA4 or NKX2-5 was added. Compound **3** did not alter the GATA4 or NKX2-5 DNA binding. Compounds **4** and **5** had a minor inhibitory effect on the NKX2-5 and GATA4 DNA binding, respectively; however, these changes were not statistically significant (Figure 3A and Figure 3B). Moreover, neonatal rat cardiomyocytes were treated with the compounds for 24 h, the nuclear proteins were extracted, and EMSA was performed. In the cardiomyocytes, compound **3** inhibited the GATA4 DNA binding by 29%, and compound **4** inhibited the GATA4 DNA binding by 37% and the NKX2-5 DNA binding by 29% (Figure 3C and Figure 3D). However, these changes were not statistically significant, suggesting that the effects of the small molecules on the GATA4- and NKX2-5-driven transcriptional synergy are not due to the inhibition or activation of the GATA4 or NKX2-5 DNA binding.

Biological Activity. The role of GATA4 in the heart ranges from the differentiation, survival, and proliferation of cardiac progenitors to the adaptive stress response, angiogenesis, and myocardial repair of the postnatal heart.[14] These diverse GATA4 functions are thought to involve differential interactions with cell-specific and signal-inducible cofactors. GATA4 and NKX2-5 are critical transcription factors that cooperatively regulate the mechanical stretch-responsive genes ANP[29] and BNP.[30] Both ANP and BNP are expressed in the developing and adult heart, and their gene expression is markedly up-regulated in response to myocyte hypertrophy and

DOI: 10.1021/acs.jmedchem.7b00816
J. Med. Chem. 2017, 60, 7781−7798

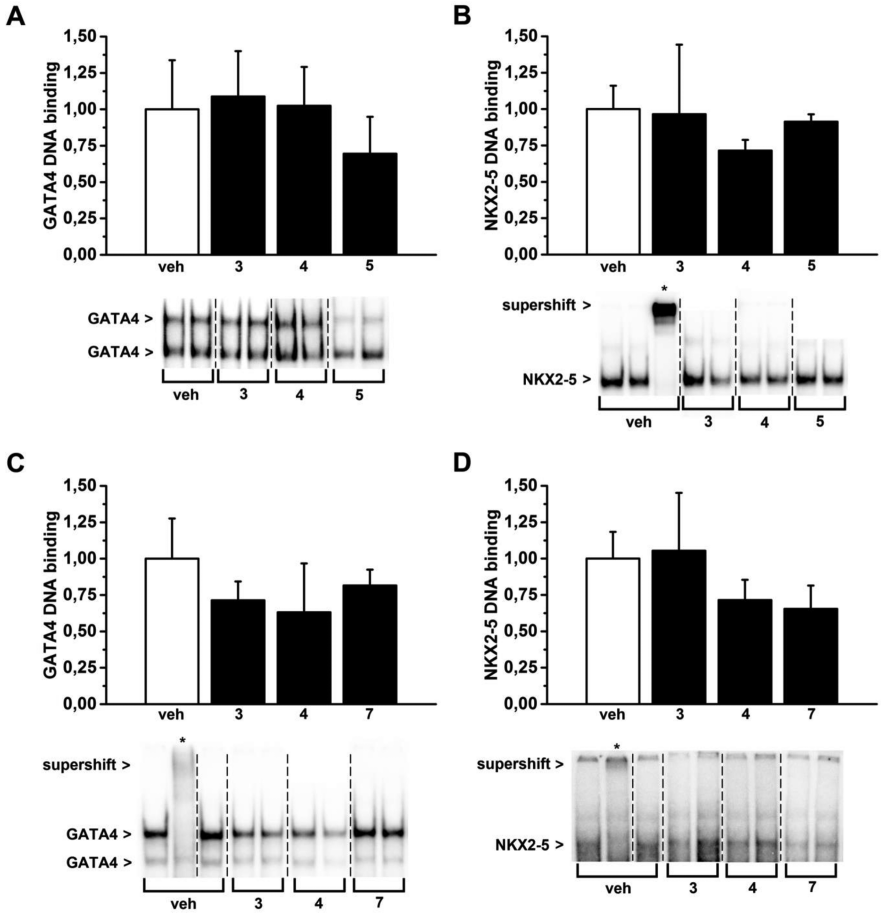

Figure 3. Effect of compounds on GATA4 and NKX2-5 protein DNA binding. (A, B) Nuclear proteins from COS-1 cells were extracted, and binding reactions and EMSA were performed as described in the Experimental Section. The concentration of the compounds **3**–**5** was 50 μM. (C, D) Neonatal rat cardiomyocytes were treated with the compounds **3**, **4**, and **7** for 24 h. Nuclear proteins were extracted, and binding reactions and EMSA were performed as described in the Experimental Section. Specific GATA4 and NKX2-5 bands are indicated. The concentration of the compounds was 50 μM. Supershift reactions were performed by incubating the reaction mixtures with anti-GATA4 and anti-NKX2-5 antibodies. Asterisks denote the lanes with the supershifted samples. The dashed line indicates where the EMSA image has been cut. The data are shown relative to the vehicle treatment as the mean ± SD, n = 3–5.

hemodynamic overload due to myocardial infarction and heart failure.[31,32] Therefore, we tested whether our newly discovered active compounds could influence ANP and BNP gene expression in vitro. Neonatal rat ventricular myocytes were treated with endothelin-1 (ET-1), which is a well-established hypertrophic agonist that activates the gene expression of both ANP and BNP,[33] and the compounds were added to the cells 1 h prior to ET-1. The compounds either augmented or inhibited the ET-1-induced gene expression of ANP and BNP (Figure 4). Consistently with the luciferase reporter gene assay finding in which compound **3** inhibited the GATA4 and NKX2-5 transcriptional synergy, compound **3** also inhibited the ET-1-stimulated BNP gene expression (68%, $p < 0.05$). There was also a tendency for compound **3** to decrease the basal mRNA levels of ANP (81%) and BNP (75%), and ET-1 stimulated the gene expression of ANP (32%), but these changes were not statistically significant (Figure 4A and Figure 4B). Compounds **8**, **9**, **10**, and **62** inhibited the ET-1-induced increase in the mRNA levels of ANP, and compound **8** also inhibited the mRNA levels of BNP (Figure 4A and Figure 4B). In contrast, compound **7**, which is an activator of the GATA4–NKX2-5 transcriptional synergy, enhanced the baseline mRNA levels of ANP (4.6-fold, $p < 0.001$) and BNP (6.4-fold, $p < 0.001$) and ET-1-stimulated gene expression of BNP (2.1-fold, $p < 0.001$) in the cardiomyocytes (Figure 4A,B). Finally, compound **4** had a mixed action, acting as an inhibitor in the transcriptional synergy assay but enhancing the basal ANP (8.6-fold, $p < 0.001$) and BNP (4.9-fold, $p < 0.001$) gene expression levels in cardiomyocytes (Figure 4A,B).

The activity of the most potent compound, i.e., compound **3**, was further validated in a cardiomyocyte hypertrophy model by utilizing cyclical stretching of ventricular myocytes. By use of this experimental model, the co-operation of GATA4 and NKX2-5 has been reported to be essential for mediating the stretch response via the NKE.[14] Myocytes were exposed to the compound at a concentration of 10 μM, and after 48 h of mechanical stretching, the myocyte area was measured. As shown in Figure 4E, compound **3** significantly inhibited the increase in the area of the myocytes in response to the stretching, indicating that the compound inhibits hypertrophic growth. Overall, the results show that the compounds can modulate the hypertrophic response in myocytes in vitro, which is consistent with the inhibition or activation of the GATA4–NKX2-5 interaction (Figures 1 and 4).

Cytotoxicity. The cytotoxicity of the selected biologically active compounds was evaluated by determining necrotic and

DOI: 10.1021/acs.jmedchem.7b00816
J. Med. Chem. 2017, 60, 7781–7798

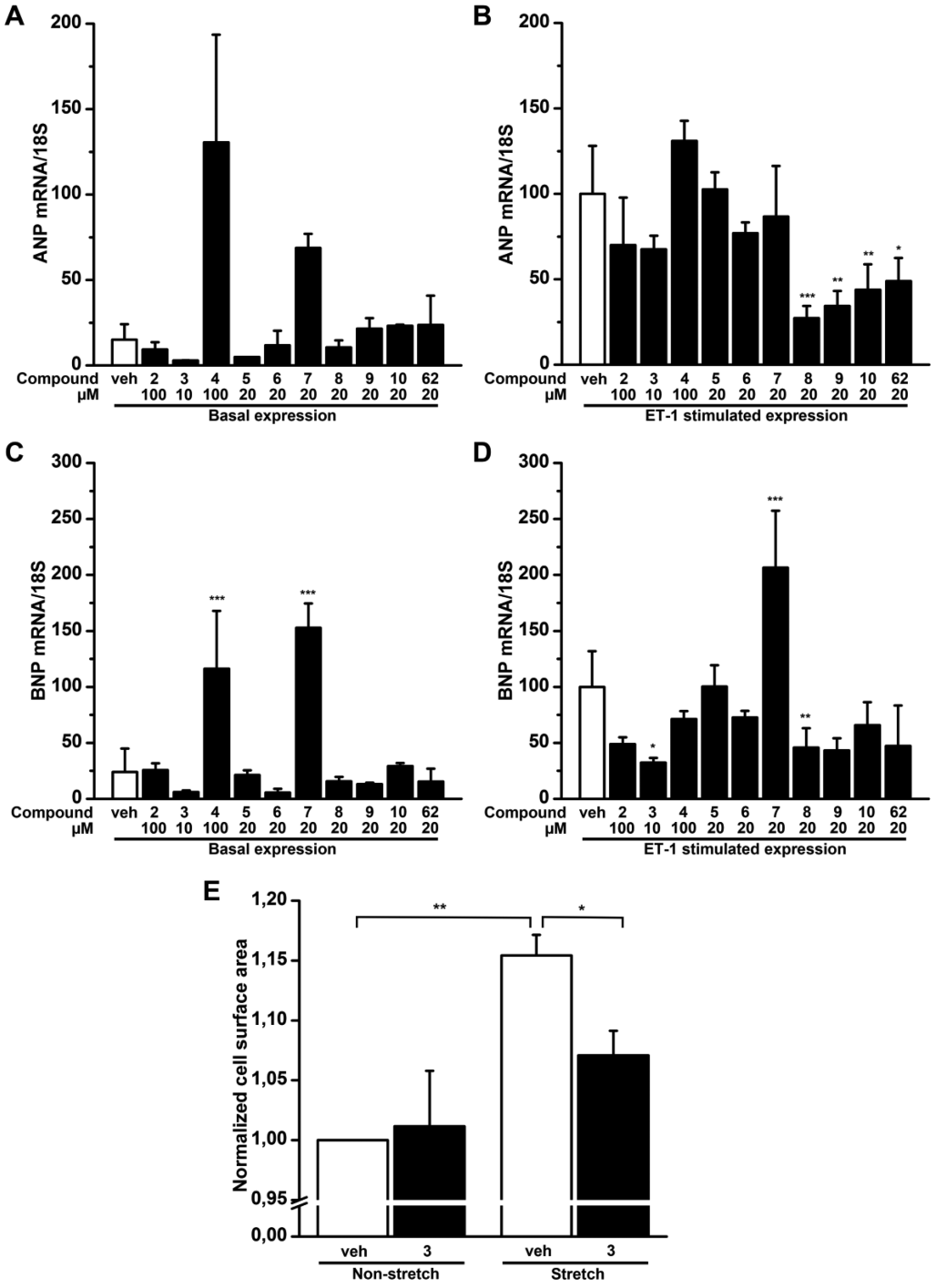

Figure 4. Effect of different compounds in the bioassays. (A–D) Neonatal rat cardiomyocytes (CMs) were treated with 100 nM endothelin-1 (ET-1) for 23 h. Compounds were added to the cells at concentrations of 10–100 μM 1 h prior to ET-1. The results are expressed as the ratio of ANP and BNP mRNA to ribosomal 18 S RNA, which were all determined by RT-PCR at 24 h. The data are shown relative to the vehicle sample as the mean ± SD: vehicle, n = 24; compounds, n = 3–6. (E) The effect of compound **3** on the hypertrophic response was investigated by exposing the CMs to 10 μM for 48 h with or without stretching. After the stretching, the CMs were fixed, stained for cardiac α-actinin, F-actin, and nuclei, and imaged under a fluorescence microscope. The surface area of the α-actinin expressing cells was determined from the images using CellProfiler software. The results are expressed as the mean of three independent experiments ± SEM: (*) $p < 0.05$, (**) $p < 0.01$, (***) $p < 0.001$ vs vehicle treatment (A–D) or appropriate group (E).

apoptotic cell death by analyzing the release of adenylate kinase (AK) and TUNEL-positive cells, respectively, in neonatal rat cardiomyocytes. The cells were treated with each compound at a concentration of 50 μM for 24 h. Compounds **3**, **4**, and **7** alone or together with ET-1 did not affect necrotic cardiomyocyte death (Figure 5A). Compounds **3**, **4**, and **7** had no effect on apoptotic cell death (Figure 5B).

Protein Kinase Profiling. To characterize the effect of the active compounds on the protein kinases, Cerep ExpresS Diversity kinase profiling was performed. Of the 48 kinases analyzed, compound **3**, at a concentration of 30 μM, inhibited

DOI: 10.1021/acs.jmedchem.7b00816
J. Med. Chem. 2017, 60, 7781–7798

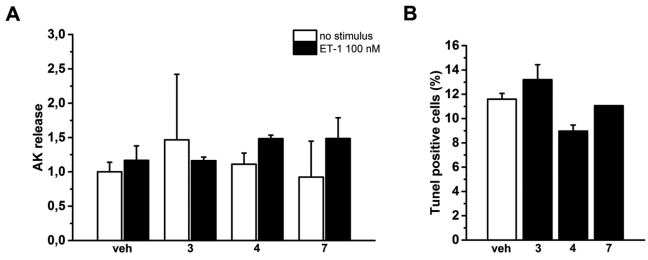

Figure 5. Cytotoxicity of compounds **3**, **4**, and **7** in neonatal rat ventricular myocytes. (A) Adenylate kinase (AK) release was determined after the cells were treated for 24 h with each compound at a concentration of 50 μM. The data are shown relative to the vehicle treatment as the mean ± SD, n = 3. (B) To detect apoptotic cells, a TUNEL assay was performed as described in the Experimental Section. TUNEL-positive cells were determined after the cells were treated for 24 h with each compound at a concentration of 50 μM. The data are shown as the mean ± SD, n = 2 (for compound **7** in TUNEL assay, n = 1).

epidermal growth factor receptor kinase (EGFR) by 54% and vascular endothelial growth factor receptor 2 kinase/kinase insert domain receptor (VEGFR2/KDR) by 64% (Table S2). In addition, compound **4** inhibited fibroblast growth factor receptor 3 kinase (FGFR3) by 55% (Table S3). It is noteworthy that compound **3** was inactive against p38α mitogen-activated protein kinase (MAPK), glycogen synthase kinase-3β (GSK-3β), extracellular signal-regulated kinase 2 (ERK2), protein kinase A (PKA), and Rho kinase 1 (ROCK1), which all have been reported to be involved in the regulation of GATA4 phosphorylation (Table S2).[13]

Cell-Based G-Protein Coupled Receptor Profiling. To test the effect of the biologically active compound **3** on 165 different G-protein-coupled receptors (GPCRs), we used Millipore GPCR profiler, which monitors calcium flux in cells expressing specific GPCR and promiscuous GPCR-coupling G$\alpha_{15/16}$ proteins. Compound **3** inhibited cannabinoid receptor type 2 (CB2), parathyroid hormone 2 receptor (PTH2), and niacin receptor 1/G-protein-coupled receptor 109A (GPR109A) with mean percentage inhibition values of 91.8, 59.5, and 58.5, respectively, but no significant agonistic effect was found (Table S4). In addition, the previously reported noncardiac inhibitory effect on ghrelin receptor was identified in this study (65.2%).[34]

Molecular Modeling. A computational analysis based on a model of GATA4−NKX2-5 bound to DNA suggests that the structural arrangement of the C-terminal extension in the second zinc finger of GATA4 plays a critical role in the transcription factor networking in the cardiac context.[35] The functional preference of GATA4 is dependent on a distinct trade-off between DNA binding and interacting with NKX2-5. Both structural arrangements are dependent on and amplified by post-translational modifications, such as phosphorylation and acetylation.[36] The evaluation of the protein structure indicates that the DNA binding of a single GATA4 partially depends on the extensive contact between the DNA and the C-terminal extension in the second zinc finger. However, our proposed GATA4−NKX2-5 interaction requires a dislocation of the loop extension, resulting in an inability of GATA4 to drive the synergy through the GATA binding site (Figure 6).

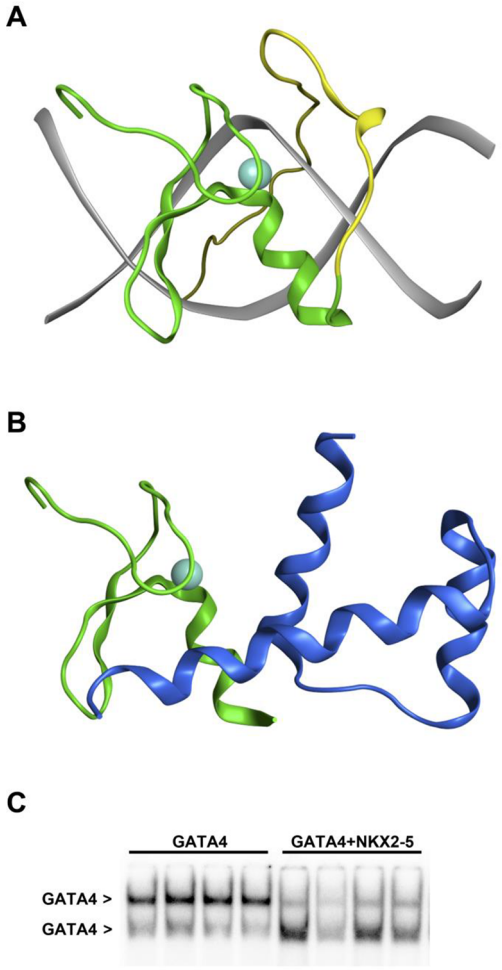

Figure 6. (A) C-terminal extension in the second zinc finger domain (yellow ribbon) contributes to the DNA binding of GATA4. (B) For the activation of the GATA4−NKX2-5 interaction, the loop extension needs to relocate and (C) enforce the structural reorganization of the GATA4 complex in the tandem GATA binding site. (C) The GATA4 and NKX2-5 proteins were overexpressed in the COS-1 cells. Nuclear proteins were extracted, and EMSA was performed as described in the Experimental Section. GATA4 alone (four parallel samples) or together with NKX2-5 (four parallel samples) was incubated in binding reactions with DNA. GATA4 binding to the rat BNP promoter (−90 bp tandem GATA site) resulted in two separate bands, and their intensities depended on the presence of NKX2-5.

■ DISCUSSION AND CONCLUSIONS

Transcription factors are the fundamental regulators of gene transcription, and many diseases, such as cancer, neurodegenerative disorders, and heart disease, are associated with the deregulation of transcriptional networks.[37] The understanding of these complex networks and pharmacological strategies that modulate the activity of distinct transcription factors will, therefore, be essential for the development of novel therapeutic approaches. A proof for the relevance of directly modulating transcription factors has been provided by targeting nuclear receptors that contain a clearly defined ligand-binding pocket and are activated by natural ligands, such as retinoic acid, glucocorticoid, estrogen or androgen receptors. Moreover, the design of small molecule drugs that interfere with transcription factor/cofactor interactions or homo-/heterodimerization between cooperating transcription factor molecules has yielded various drugs that are capable of counteracting

DOI: 10.1021/acs.jmedchem.7b00816
J. Med. Chem. 2017, 60, 7781−7798

Scheme 3. Transcriptional Activity of GATA4 Is Regulated by Interactions with Several Other TFs and Post-Translational Modifications[13,17−19,a]

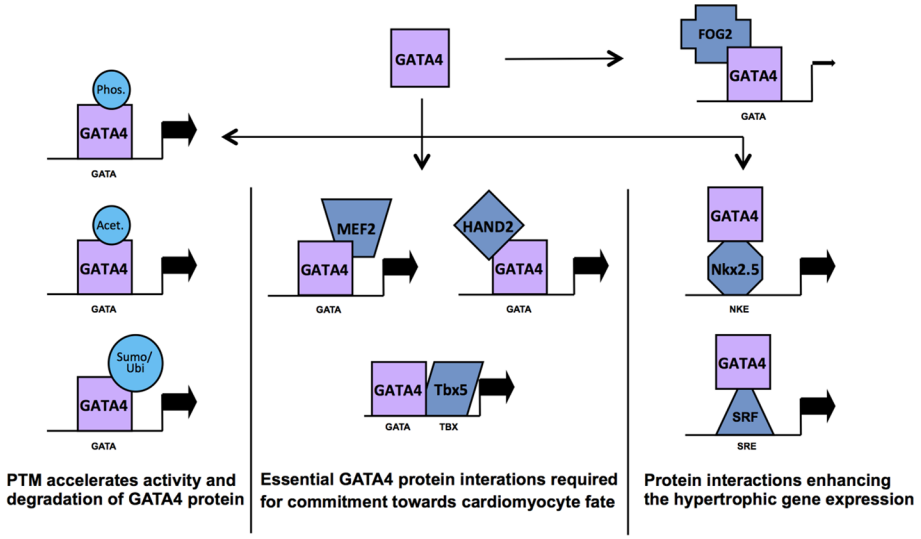

[a]Most of the protein−protein interactions of GATA factors are mediated by the C-terminal zinc finger, while the N-terminal zinc finger interacts with Friend of GATA (FOG) transcription factors. Selected heterotypic interactions and DNA occupation modes for GATA4 are classified based on experimental measurements of the binding preferences.[25,42−46] Heterotypic GATA4 complex subpopulations have distinct context dependent effects on the commitment of stem cells toward the cardiac fate or the enhancement of hypertrophic gene expression in mature cardiac cells. SRF, serum response factor; SRE, serum response element; PTM, post-translational modification; Phos, phosphorylation; Acet, acetylation; Sumo/Ubi, sumoylation/ubiquitination.

specific DNA-regulatory proteins.[38] Thus, protein−protein interactions of key transcription factors are likely to present one of the next major classes of innovative therapeutic targets.

A substantial body of evidence suggests that a limited number of regulatory transcription factors (e.g., GATA4, HAND2, MEF2, NKX2-5, and TBX5) are needed for the initiation of cardiac-like gene expression.[20,39−41] Investigations of heterotypical interactions involving GATA4 have revealed that transcription factors that are critical for cardiac reprogramming, such as MEF2,[42] HAND2,[43] and TBX5,[44,45] tend to synergistically activate the GATA binding site (Scheme 3). In contrast, the overexpression of either NKX2-5[25] or SRF[46] leads to protein complex formation and, consequently, the activation of their corresponding sites with a diminished ability to drive cardiac transdifferentiation.[47] In addition to the GATA4−TBX5 interaction, other heterotypic GATA4 protein interactions require only a single binding element at the promoter. Overall, previous studies suggest that NKX2-5 plays both a structural[15] and functional[16] role as a dominant cofactor of GATA4. Since an orchestrated and sequential expression of transcription factors is essential for the development of cardiac cells, theoretically, the inhibition of the GATA4−NKX2-5 protein complex would result in other GATA4-associated TF combinations that would more efficiently program cells toward a cardiomyocyte fate (Scheme 3). Interestingly, the increased research efforts targeting nuclear receptors have revealed that the interaction between GATA4 and NKX2-5 shares the same architecture as the two zinc fingers in the DNA binding domain of nuclear receptors,[15] implicating that small molecules have ability to modulate the GATA4 and NKX2-5 protein−protein interactions.

In the present study, we identified four small molecule families that produce either an agonistic or antagonist effect on the GATA4−NKX2-5 transcriptional synergy. Here, we used the NKE site to study the GATA4−NKX2-5 cooperative interaction. The 3xNKE reporter is an artificial tool used to detect the more pronounced signal from the GATA4−NKX2-5 synergy for screening purposes. Moreover, it has been shown that the NKE site is essential for the GATA4−NKX2-5 cooperation in stretching-induced hypertrophy.[14] A fragment-based screening, transcriptional synergy measuring reporter gene assay, and pharmacophore search were utilized for the small molecule screening, identification, and optimization. The primary screening using a reporter gene assay and the in vitro cell culture studies revealed several biologically active compounds, i.e., **3**, **4**, **5**, **6**, and **7**, with distinct profiles. The structure−activity relationship studies of inhibitory compounds **3**, **4**, and **5** demonstrated the indispensable role of the two heavy atom linker together with a hydrogen acceptor feature next to the five-member ring, while a completely opposite agonistic effect was achieved by introducing a substituted five-member ring into the amide bond (**7**). In the cardiomyocyte cultures, the compounds either augmented or inhibited the hypertrophic agonist-induced ANP and BNP expression. In addition, the GPCR and kinase screenings with the most potent compound, i.e., **3**, *N*-[4-(diethylamino)phenyl]-5-methyl-3-phenylisoxazole-4-carboxamide, did not detect cross-linking pathways with the major cardiac signaling cascades. Compound **3** and its derivatives may provide a new class of small molecules for modulating cardiogenesis and heart regeneration (Scheme 3). Even though the precise binding site of the tool compounds in the GATA4−NKX2-5 interaction remains to be established, the structural similarity and spatial appearance suggest the existence of a common binding site that mediates the actions of the active compounds. Of note, the results concerning particular compounds may include unspecific effects, i.e., the high concentration of compound **4** in the ET-1 assay, the context-dependent degradation of the ester structure with compound **5**, and the frequent binder characteristic of compound **6**.[48,49]

DOI: 10.1021/acs.jmedchem.7b00816
J. Med. Chem. 2017, 60, 7781−7798

Previously, numerous small molecule-based approaches have been shown to enhance cardiac reprogramming, including the activation of Wnt/β-catenin signaling (GSK3β inhibitors), inhibition of Wnt-signaling (porcupine and tankyrase inhibitors), or modulation of transforming growth factor (TGF) β-superfamily signaling (bone morphogenetic protein and TGFβ inhibitors).[50,51] These signaling pathways are essential during the early phases of cardiac differentiation (mesoderm induction).[52] The combined application of Wnt- and TGFβ-modulators requires strict time-dependent dosing in cellular assays to yield optimal conditions for cardiac reprogramming. Nevertheless, systematic protocol optimizations have led to a powerful platform for cardiac differentiation from human pluripotent stem cells using small molecule modulators of Wnt-signaling.[53] Additionally, very recently, Cao et al. and Mohamed et al. presented pharmacological lineage-specific approaches for the efficient conversion of human fibroblasts into functional cardiomyocytes using either a combination of nine small molecules[54] or TGFβ- and Wnt-inhibitors jointly with three cardiac transcription factors, i.e., GATA4, MEF2c, and TBX5.[55] However, the translation of the in vitro tool compounds to in vivo candidates for cardiac regeneration is challenging, e.g., requires the optimization of the physicochemical or ADME properties that is necessary for efficacy in vivo. Moreover, although the in vivo dosing of tool compounds that regulate Wnt- or TGFβ-signaling may interfere with the pathways beneficial for cardiac regeneration, these compounds are potentially pro-oncogenic.[50]

Regarding the cardiac transcription factors, Sadek et al. performed a small molecule library screening for chemical activators of *NKX2-5*, which is one of the earliest lineage-restricted genes to be expressed in cardiovascular progenitor cells.[56] A chemical library of 147 000 compounds was screened in P19CL6 cells harboring an NKX2-5 luciferase reporter construct, which led to the identification of 10 potential molecular scaffolds with cardiogenic activity, including lead compounds, such as sulfonylhydrazones (Shz-1) and isoxazoles (Isx-9). Moreover, mechanistic follow-up studies suggest that both Shz-1 (activation of Brachyury T together with early cardiogenic program genes, such as NKX2-5 and myocardin[56]) and Isx-9 (agonist of orphan GPR68, which is an extracellular proton/pH sensing GPCR[57]) act independently of the known procardiogenic pathways, such as Wnt and the TGFβ superfamily. Of note, although various active molecular scaffolds identified by Sadek et al. share similarities with the compounds in the present study, including 3,5-disubstituted isoxazoles vs 3,4,5-trisubstituted isoxazoles, thiazolidinediones, and flavonoids, Isx-9 did not inhibit the luciferase reporter gene activity in our GATA4−NKX2-5 transcriptional synergy assay (data not shown).

In conclusion, adult cardiomyocytes are terminally differentiated, and their capacity for renewal is limited in response to cardiac injury.[58] A core set of transcription factors control the direct reprogramming of fibroblasts into induced cardiomyocytes[41,59−61] and directed differentiation of stem cells[62,63] and are, therefore, implicated as potential novel drug targets for heart regeneration.[39] One attractive strategy is to inhibit the protein−protein interaction since many transcription factors act as homo- or heterodimers and depend on cofactors to function appropriately.[36] Our results (3xNKE reporter assay, BNP transcription, endothelin-1 stimulated gene expression of ANP and BNP, hypertrophic cell surface growth in cardiomyocytes, and immunoprecipitation assay) provide evidence of the small molecule-mediated modulation of the transcriptional synergy between GATA4 and NKX2-5, which plays essential roles in programming cells toward the cardiomyocyte fate and mediating the stretching-induced hypertrophic response. GATA4 is also a critical regulator of biological processes in myocardial remodeling and repair.[13] However, the inhibitory compounds could alter the interaction between GATA4 and other binding partners, and thus a more detailed assessment and validation of the molecular mechanism(s) and the optimization of small molecules are needed to fully evaluate the potential of GATA4−NKX2-5 interaction modulators in chemically mediated cardiogenesis and heart repair and regeneration.

EXPERIMENTAL SECTION

Homology Modeling and Sequence Alignment. A homology model of GATA4 was constructed using the highly conserved C-terminal zinc finger domain of GATA3 as a template structure (Protein Data Bank code 3DFX, sequence identity 76%) for the C-terminal zinc finger of GATA4. A homology model for the homeodomain of NKX2-5 was built using the homeodomain of the related thyroid transcription factor 1 as a template structure (Protein Data Bank code 1FTT, sequence identity 61%). Other than the C- and N-terminal domains, template structures are lacking and were, therefore, excluded from the modeling. The sequence alignments were constructed without any insertions or deletions using PSI-BLAST. The commercial modeling package Molecular Operating Environment (MOE 2014.09; Chemical Computing Group Inc., Montreal, Canada; www.chemcomp.com) was used to construct the homology models of the protein domains. An AMBER99 force field was applied as the source of the atom parameters for the protein minimizations and scoring during the homology modeling. The side chain data parameters were assembled from the extensive MOE-integrated rotamer library. During the homology modeling, 10 protein domain specific intermediate models were generated using the Boltzmann-weighted randomized modeling procedure. All intermediate models were submitted to an electrostatic-enabled energy minimization calculation until the root mean square (rms) gradient fell below 1. Subsequently, the refined protein models were scored using the generalized Born/volume integral (GB/VI) methodology.[64] The highest scoring intermediate model was further minimized until the rms fell below 0.5 and, subsequently, was selected as the final model. The refined final models were inspected (bond lengths, bond angles, atom clashes, and contact energies) and confirmed to have satisfactory stereochemical quality using Ramachandran plots (φ and ψ angles).[65]

In Silico Fragment Screening. Binding site assessments of the homology models of GATA4 and NKX2-5 were carried out using the MOE-integrated Alpha Site Finder calculation using the default settings. Multiple copy simultaneous chemical probe analyses[27] were applied to the highest ranked binding pocket of the rigid GATA4 protein. MMFF94 was selected as the appropriate force field for the receptor−ligand interactions. The DNA binding site of the GATA4 protein model was exposed to a collection of 39 randomly placed molecular fragments and, subsequently, an energy minimization to rank the interaction potential (with and without the solvent) of the fragments with diverse functional groups inside the proposed binding cavity. The default settings and protocols were applied to the fragment library, number of fragment copies, energy minimization termination gradient, and protein flexibility parameters.

Pharmacophore Preparation and Search. A flexible molecular alignment was implemented to study the 3D molecular similarity to elucidate the common pharmacophoric query of the three active compounds (**3**, **4**, and **5**). The stochastic search procedure aligns the conformational space of the molecules by maximizing the molecules' chemical similarity with the least amount of internal strain. An Amber12:EHT force field was applied for the molecule parametrizations and energy minimizations. Furthermore, the default

DOI: 10.1021/acs.jmedchem.7b00816
J. Med. Chem. 2017, 60, 7781−7798

settings were employed to score and rank the collection of compound superpositions.[66] The best-ranking alignment of active compounds was utilized to generate the pharmacophore annotation points (four point pharmacophore with two acceptor, aromatic, and hydrophobic features). Excluded volume constraints derived from the GATA4 protein model were utilized as a shape restrictor in the pharmacophore query. The MOE conformation database (650 000 leadlike compounds from 44 chemical suppliers) was used as a ligand reservoir for the pharmacophore search.

Screening of Commercial Small Molecules. Small molecules for the primary screening and luciferase reporter gene assay based optimization were selected and purchased from established suppliers, including ChemBridge (San Diego, CA, USA), Enamine (Kiev, Ukraine), Sigma-Aldrich (St. Louis, MO, USA), and Specs (Zoetermeer, The Netherlands). All compounds purchased for the study were tested by HPLC−MS and ^{1}H NMR by the vendors to confirm the sample identity and ensure a minimum purity of 90%.

Chemistry. The synthesis of selected compounds (i.e., **3**, **4**, **7**, **31**, and **32**) were outsourced to Pharmatory (Oulu, Finland). All reactions were carried out with commercially available solvents and chemicals. All chemicals, solvents, and anhydrous solvents were acquired from Sigma-Aldrich (Schnelldorf, Germany), Fluka (Buchs, Switzerland), and Alfa Aesar (Ward Hill, MA, USA). The purity of the final compounds was determined by HPLC/MS and ^{1}H NMR (minimum purity >95%). The ^{1}H NMR spectra were observed at the University of Oulu using a Bruker DPX 200 instrument (Rheinstetten, Germany) in $CDCl_3$ or DMSO-d_6. The reported chemical shifts (δ) are expressed in parts per million (ppm), and the coupling constants (J) are expressed in hertz (Hz). The spin multiplicities are reported as s = singlet, br s = broad singlet, d = doublet, t = triplet, q = quartet, m = multiplet, and br = broad.

The HPLC−MS analysis was performed on an Agilent Technologies 1100 HPLC fitted with Hewlett-Packard series 1100 MSD with Zorbax Extend-C18 150 mm × 4.6 mm, 5 μm, 30 °C, and water + 0.20% v/v trifluoroacetic acid and acetonitrile as the eluent. The HPLC analyses were performed on Zorbax Extend-C18 150 mm × 4.6 mm, 5 μm at an ambient temperature using water + 0.20% v/v trifluoroacetic acid and acetonitrile as the eluent.

General Synthetic Procedure for Manufacturing Compound 3 and Other Relative Compounds. One equivalent of a suitably 3,5-disubstituted isoxazole-4-carboxylic acid is dissolved in a solvent, such as DMF, and the obtained solution is cooled to 0−10 °C. One equivalent of a suitably substituted benzene-amine and an excess of *O*-(benzotriazol-1-yl)-*N*,*N*,*N*′,*N*′-tetramethyluronium tetrafluoroborate (TBTU) are added, and the mixture was stirred at 0−10 °C for 5−30 min. An excess of a non-nucleophilic base, such as diisopropylethylamine, is slowly added, and the mixture is stirred at 0−10 °C for 2−5 h. Depending on the substituents used, either isoxazole-carboxylic acid or benzene-amine, or both, can be modified by introducing suitable protective groups to the selected substituents prior to their reaction to yield the product compound.

An organic solvent of a suitable polarity, such as ethyl acetate and an aq $NaHCO_3$ solution, is added to the reaction mixture to dissolve the compound, and the mixture is stirred at an ambient temperature until dissolution occurs. The layers are separated, and the organic phase is washed with water (e.g., 3 times) and brine (e.g., once). The organic layer is then dried using a drying agent, such as sodium sulfate. The drying agent is then filtered, and the solution is evaporated to dryness to yield the crude compound.

The crude compound can be purified by dissolving it at a temperature of 25−70 °C in a solvent of a suitable polarity, such as ethyl acetate, and stirring the solution. An activated carbon can optionally be added, and the mixture stirred and filtered through Celite, whereby some impurities can be removed. Finally, precipitation of the product can be achieved by cooling the solution to a point at which it begins to crystallize or adding a second solvent with a polarity opposite that of the first solvent, such as *n*-heptane, to the previous solution and slowly cooling the mixture to a point at which the product begins to crystallize. The pure precipitated product can then be filtered, washed with the second solvent (e.g., twice), and dried, optionally under vacuum.

***N*-[4-(Diethylamino)phenyl]-5-methyl-3-phenylisoxazole-4-carboxamide (3).** 5-Methyl-3-phenylisoxazole-4-carboxylic acid (8.00 g, 39.4 mmol) was dissolved in DMF (200 mL), and the solution cooled to 0−10 °C. *N*′,*N*′-Diethylbenzene-1,4-diamine (6.47 g, 39.4 mmol) and TBTU (15.17 g, 47.3 mmol) were added, and the mixture was stirred at 0−10 °C for 10 min. Diisopropylethylamine (6.11 g, 47.3 mmol) was slowly added, and the mixture was stirred at 0−10 °C for 2.5 h. Ethyl acetate (400 mL) and a 5% aq $NaHCO_3$ solution (160 mL) were added to the reaction mixture, and the mixture was stirred at an ambient temperature for 15 min. The layers were separated, and the organic phase was washed with water (3 × 200 mL) and brine (180 mL). The organic layer was dried with sodium sulfate, the drying agent was filtered, and the solution evaporated to dryness to yield 12.8 g of crude compound **3**. The crude compound was dissolved in warm ethyl acetate (300 mL), and activated carbon (0.5 g) was added. The mixture was stirred for 20 min and filtered through Celite. *n*-Heptane (120 mL) was added to the previous solution at 55 °C, and the mixture was slowly cooled to 0−5 °C. The precipitated product was filtered, washed with *n*-heptane (2 × 50 mL), and dried under vacuum at 45 °C overnight to yield 8.52 g (62%) of compound **3** as an off-white powder. NMR: 10.12 ppm (s, 1H, NH), 7.71 ppm (m, 2H, arom), 7.35−7.50 ppm (m, 5H arom), 6.63 ppm (d, 2H, arom), 3.30 ppm (q, 4H, 2 × CH_2), 2.55 ppm (s, 3H, CH_3), 1.05 ppm (t, 6H, 2 × CH_3). MS: m/z 350.2 (100%, M + 1), 351.2 (25%). Melting point range: 139.3−140.2 °C.

4-[(4-Propoxybenzylidene)amino]-5-(pyridin-4-yl)-4*H*-1,2,4-triazole-3-thiol (4). A mixture of 4-propoxybenzaldehyde (10.00 g, 60.9 mmol) and 4-amino-5-(pyridin-4-yl)-4*H*-1,2,4-triazole-3-thiol (11.8 g, 60.9 mmol) in glacial acetic acid (100 mL) was heated to reflux for 2.5 h, and the solution was filtered hot. The filtrate was allowed to cool to an ambient temperature and was then cooled further to 5 °C with an ice bath. The precipitated product was filtered, washed with acetic acid (3 × 20 mL), and dried with suction to yield 17.8 g of crude compound **4**. Crude compound **4** was dissolved in boiling glacial acetic acid (110 mL), and the solution was allowed to slowly cool to an ambient temperature. The precipitated product was filtered, washed with acetic acid (2 × 10 mL) and water (2 × 10 mL), and dried under vacuum at 40 °C for 8 h to yield 12.0 g (58%) of compound **4**. NMR (DMSO-d_6): 9.51 ppm (s, 1H, SH), 8.75 ppm (m, 2H, arom), 7.88 ppm (m, 4H arom), 7.11 ppm (d, 2H, arom), 4.04 ppm (t, 2H, CH_2), 1.76 ppm (m, 2H, CH_2), 0.98 ppm (t, 3H, CH_3). MS: m/z 340.1 (100%, M + 1), 341.1 (22%), 362.0 (5%, M + Na). Melting point: decomposition.

***N*-(4-Chlorophenyl)-5-methyl-*N*-(4-methyl-4,5-dihydrothiazol-2-yl)-3-phenylisoxazole-4-carboxamide (7).** 5-Methyl-3-phenylisoxazole-4-carboxylic acid (1.01 g, 4.97 mmol) was dissolved in DMF (25 mL), and the solution was cooled to 0−10 °C. *N*-(4-Chlorophenyl)-4-methyl-4,5-dihydrothiazol-2-amine (1.12 g, 4.94 mmol) and TBTU (1.90 g, 5.92 mmol) were added, and the mixture was stirred at 0−10 °C for 10 min. Diisopropylethylamine (0.78 g, 6.04 mmol) was slowly added, and the mixture was stirred at 0−10 °C for 4 h. The cooling bath was removed, and the mixture was stirred for an additional 50 min, allowing it to warm to an ambient temperature. Ethyl acetate (40 mL) and 10% aq $NaHCO_3$ solution (35 mL) were added to the reaction mixture, and the mixture was stirred at an ambient temperature for 5 min. The layers were separated, and the organic layer was washed with water (3 × 30 mL) and brine (15 mL). The organic layer was dried with sodium sulfate, the drying agent was filtered, and the solution was evaporated to dryness to yield 2.20 g of crude compound **7**. The crude material was dissolved in ethyl acetate (10−12 mL) at an ambient temperature, and the solution was stirred at an ambient temperature for 15 min; during this time, the product began to crystallize out of the solution. *n*-Heptane (20 mL) was added, and the mixture was stirred at an ambient temperature for 15 min; during this period, more of the product precipitated. The precipitated product was filtered, washed with *n*-heptane, and dried under vacuum at 50 °C overnight to yield 1.53 g of compound **7** as a white powder. NMR ($CDCl_3$): 7.35−7.60 ppm (m, 5H, arom), 7.08−7.18 ppm (m,

DOI: 10.1021/acs.jmedchem.7b00816
J. Med. Chem. 2017, 60, 7781−7798

2H, arom), 6.31−6.43 ppm (m, 2H arom), 3.50−4.20 ppm (broad m, 2H thiazole CH_2), 3.57 ppm (m, 1H, thiazole CH), 2.59 ppm (s, 3H, CH_3), 1.36 ppm (d, 3H, thiazole CH_3). Melting point range: 145.6−147.3 °C.

***N*-[4-(Ethylamino)phenyl]-5-methyl-3-phenylisoxazole-4-carboxamide (31).** 5-Methyl-3-phenylisoxazole-4-carboxylic acid (300 mg, 1.48 mmol) was dissolved in DMF (7.5 mL), and the solution was cooled to 0−10 °C. 1-*N*-Ethylbenzene-1,4-diamine (201 mg, 1.48 mmol) and TBTU (569 mg, 1.77 mmol) were added, and the mixture was stirred at 0−10 °C for 10 min. Diisopropylethylamine (0.30 mL, 1.77 mmol) was slowly added, and the mixture was stirred at 0−10 °C for 1.5 h. Ethyl acetate (30 mL) and 5% aq $NaHCO_3$ solution (30 mL) were added to the reaction mixture, and the mixture was stirred at an ambient temperature for 15 min. The layers were separated, and the aqueous layer was washed with ethyl acetate (15 mL). The combined organic solutions were washed with water (30 mL) and brine (20 mL). The precipitated product was filtered and dried under vacuum at 30 °C for 20 h to yield 282 mg of compound **31** as a pinkish powder. NMR (DMSO-d_6): 10.05 ppm (s, 1H, NH), 7.71 ppm (m, 2H, arom), 7.50 ppm (m, 2H arom), 7.32 ppm (d, 2H arom), 6.52 ppm (d, 2H, arom), 5.43 ppm (t, 1H, NH), 3.00 ppm (m, 2H, CH_2), 2.55 ppm (s, 3H, CH_3), 1.14 ppm (t, 3H, CH_3). MS: *m*/*z* 322.1 (100%, M + 1), 344.2 (25%, M + Na). Melting point range: 203.1−205.9 °C.

***N*-[4-(Ethylamino)phenyl]-5-(hydroxymethyl)-3-phenylisoxazole-4-carboxamide (32).** *Step 1*. Magnesium ethoxide (4.85 g, 42.4 mmol) was suspended in dry toluene (9 mL), and ethyl benzoyl acetate (7.40 g, 38.5 mmol) was added. After stirring the reaction mixture for 1 h at room temperature, dry acetonitrile (9 mL) was added, and the reaction mixture was cooled to −10 °C. Chloroacetyl chloride (4.78 g, 3.37 mL, 42.4 mmol) was added for 35 min. The reaction mixture was allowed to warm to room temperature and stirred for 1 h. Sulfuric acid (1 mL) in ice−water (35 mL) was added to the mixture, and the layers were separated. The aqueous layer was washed with diethyl ether (20 mL), and the combined organic layers were dried with magnesium sulfate. The drying agent was filtered, and the filtrate was cooled to 0 °C. Triethylamine (5.4 mL) was dissolved in diethyl ether (3 mL), and the mixture was added to the filtrate. The reaction mixture was then stirred at room temperature for 40 min. The precipitated triethylamine hydrochloride was filtered, and the solution was evaporated to dryness to yield 9.74 g (109%) of crude ethyl 2-oxo-4-phenyl-2,5-dihydrofuran-3-carboxylate (intermediate **1**), which was used in the next step without further purification.

Step 2. The crude intermediate **1**, which was prepared as described above (9.74 g), was dissolved in ethanol (39 mL), and hydroxylamine hydrochloride (2.68 g, 38.5 mmol) and potassium acetate (3.78 g, 38.5 mmol) were added. The reaction mixture was heated to reflux for 40 min and then cooled to room temperature. Ethanol was removed by evaporation under reduced pressure, and water (77 mL) was added to the evaporation residue. The product was extracted with diethyl ether (2 × 20 mL), and the combined organic layers were washed with brine and dried with magnesium sulfate. The drying agent was filtered, and the filtrate was evaporated to dryness under reduced pressure to yield 9.07 g (97% over two steps) of crude ethyl 5-(hydroxymethyl)-3-phenylisoxazole-4-carboxylate (intermediate **2**). NMR ($CDCl_3$): 7.35−7.65 ppm (m, 5 H, arom), 4.95 ppm (s, 2H, CH_2), 4.26 ppm (q, 2 H, CH_2), 1.20 ppm (t, 3H, CH_3).

Step 3. Crude intermediate **2** (1.0 g, 4.04 mmol) was dissolved in dichloromethane (28 mL) and 3,4-dihydro-2*H*-pyran (0.51 g, 6.07 mmol), and pyridinium *p*-toluenesulfonate (0.10 g, 0.4 mmol) was added. The reaction mixture was stirred at room temperature for 6 h. The reaction mixture was diluted with dichloromethane (20 mL) and washed with half-diluted brine (40 mL). The organic layer was dried with magnesium sulfate, the drying agent was filtered, and the filtrate was evaporated to dryness to yield 1.38 (103%) of crude ethyl 3-phenyl-5-(((tetrahydro-2*H*-pyran-2-yl)oxy)methyl)isoxazole-4-carboxylate (intermediate **3**), which was used without further purification.

Step 4. The crude intermediate **3** (1.30 g, 3.92 mmol), which was prepared as described above, was dissolved in methanol (39 mL), and cesium carbonate (2.56 g, 7.85 mmol) was added. The reaction mixture was stirred at an ambient temperature over the weekend. The solution was evaporated to dryness under reduced pressure, and the residue was divided between ethyl acetate (20 mL) and water (20 mL). The pH of the aqueous layer was adjusted to pH 2 with 37% aq HCl, and the layers were separated. The aqueous layer was washed with ethyl acetate (20 mL), the combined organic layers were dried with magnesium sulfate, and the organic solution was evaporated to dryness to yield 1.03 g (87%) of crude 3-phenyl-5-(((tetrahydro-2*H*-pyran-2-yl)oxy)methyl)isoxazole-4-carboxylic acid (intermediate **4**). NMR ($CDCl_3$): 8.19 ppm (broad s, 1H, COOH), 7.30−7.75 ppm (m, 5 H, arom), 5.09 ppm (q, 2H, CH_2), 4.49 ppm (m, 1H, CH), 3.91 ppm (m, 1H, CH_2), 3.61 ppm (m, 1H, CH_2), 1.35−1.95 ppm (m, 6H, CH_2).

Step 5. Intermediate **4** (450 mg, 1.48 mmol) was dissolved in DMF (12 mL), and the solution cooled to 0−10 °C. 1-*N*-Ethylbenzene-1,4-diamine (220 mg, 1.62 mmol) and TBTU (577 mg, 1.80 mmol) were added, and the mixture was stirred at 0−10 °C for 10 min. Diisopropylethylamine (0.30 mL, 1.77 mmol) was slowly added, and the mixture was stirred at 0−10 °C for 1.5 h. Ethyl acetate (40 mL) and 5% aq $NaHCO_3$ solution (30 mL) were added to the reaction mixture, and the mixture was stirred at an ambient temperature for 15 min. The precipitated product was filtered, washed with ethyl acetate, and dried to yield 560 mg (89%) of *N*-(4-(ethylamino)phenyl)-3-phenyl-5-(((tetrahydro-2*H*-pyran-2-yl)oxy)methyl)isoxazole-4-carboxamide (intermediate **5**), which was used in the final deprotection step. NMR (DMSO-d_6): 10.15 ppm (s, 1H, NH), 7.74 ppm (m, 2H, arom), 7.52 ppm (m, 3H arom), 7.32 ppm (d, 2H arom), 6.52 ppm (d, 2H, arom), 5.44 ppm (t, 1H, NH), 4.82 ppm (q, 2H, CH_2), 4.7 ppm (m, 1H, CH), 3.72 ppm (m, 1H, CH_2), 3.45 ppm (m, 1H, CH_2), 3.00 ppm (q, 2H, CH_2), 1.30−1.80 ppm (m, 6H, CH_2), 1.00 ppm (t, 3H, CH_3).

Compound **32**. Intermediate **5** (70 mg, 0.17 mmol) was dissolved in THF (1.4 mL), the pH of the solution was adjusted to pH 3 with 2 M aq HCl solution, and the reaction mixture was stirred at an ambient temperature overnight. The temperature of the solution was then adjusted to 50 °C, and the stirring continued for 2 h. The pH was adjusted to 9−10 with 5 M aq NaOH solution, and water (5 mL) was added. The mixture was extracted with ethyl acetate (3 × 5 mL), and the combined organic layers were washed with water (3 × 3 mL), dried over sodium sulfate, and evaporated to dryness to yield 57 mg (102%) of crude compound **32**. The crude product was purified by chromatography using ethyl acetate−heptane 1:1 as the eluent to yield 39 mg (71%) of compound **32**. NMR (DMSO-d_6): 10.07 ppm (s, 1H, NH), 7.71 ppm (m, 2H, arom), 7.51 ppm (m, 3H arom), 7.31 ppm (d, 2H arom), 6.52 ppm (d, 2H, arom), 5.88 ppm (t, 1H, OH), 5.43 ppm (t, 1H, NH), 4.71 ppm (d, 2H, CH_2), 3.00 ppm (q, 2H, CH_2), 1.14 ppm (t, 3H, CH_3). MS: *m*/*z* 338.1 (100%, M + 1), 360.2 (25%, M + Na).

Technique for the Detection of Aggregation. The compounds of interest (i.e., compounds **3**, **4**, and **7**) were diluted in DMSO to obtain a stock of 100 mM, which was further diluted with DMSO to obtain four different concentrations (100, 30, 10, and 3 mM). From these concentrations 1 μL of solution was diluted to 1 mL of Dulbecco's modified Eagle's medium (DMEM, Sigma-Aldrich/Gibco) containing 10% fetal bovine serum (FBS, Gibco) and 1% penicillin−streptomycin (PS, Sigma-Aldrich) (100 U/mL and 0.1 mg/mL, respectively) referring the same conditions as in cell culture. Finally, an amount of 100 μL of this solution was transferred to a 96-well microplate (BRANDplates pureGrade). The final concentrations (i.e., 100, 30, 10, and 3 μM) were in 0.1% DMSO. For the measurements, DMEM with FBS and PS and 0.1% DMSO were used as a blank to account for any signals due to the assay conditions. The blank and all four concentrations of the samples were measured as triplicates at three different voltages (300, 400, and 500 V) using a Nepheloskan Ascent by Labsystems (Helsinki, Finland).

In Vitro Chemical Stability of Compound 3. HPLC−MS CHROMASOLV grade chloroform, acetonitrile, formic acid, and sodium chloride were obtained from Sigma (Darmstadt, Germany). Water was freshly prepared in-house with a Milli-Q (Millipore Oy, Espoo, Finland) purification system and was ultrapure grade (18.2 MΩ).

DOI: 10.1021/acs.jmedchem.7b00816
J. Med. Chem. 2017, 60, 7781−7798

Extraction Method for the Extracellular (Cell Culture Media) Metabolites. Eight samples with no cells were thawed at room temperature, and compound **3** was extracted from the cell culture media with 500 μL of chloroform. The samples were vortexed briefly and centrifuged at 16 000 rpm at 4 °C for 10 min. The bottom chloroform layer was transferred to a glass vial and analyzed by UPLC−ESI(+)-QTOF/MS in the sensitivity mode.

Extraction Method for the Intracellular Metabolites. Eight samples with cell culture media and mouse embryonic stem cells were thawed on ice and centrifuged at 16 000 rpm at 4 °C for 10 min. The supernatants were removed, and cells were washed twice with 200 μL of 0.9% saline (H_2O), followed by centrifugation at 16 000 rpm at 4 °C for 10 min. The washed cells were disrupted, and compound **3** was extracted with 200 μL of chloroform in an ultrasonic bath for 10 min, followed by centrifugation at 16 000 rpm at 4 °C for 10 min. The bottom chloroform phase was transferred to a glass vial and analyzed by UPLC−ESI(+)-QTOF/MS in the sensitivity mode.

Analytical Method. A Waters Acquity ultraperformance liquid chromatographic (UPLC) system (Waters Corp., Milford, MA, USA) with an autosampler, vacuum degasser, and column oven was used. The analytical column used was a Waters Acquity BEH C18 (2.1 mm × 50 mm, 1.7 μm, Waters Corp, Milford, MA, USA), together with an online filter. The used eluents were 0.1% formic acid in H_2O (A) and 0.1% formic acid in acetonitrile (B). A linear gradient elution of 7% B−80% B was applied for 5 min, followed by 1 min of column equilibration. The flow rate was 0.6 mL/min, and the column oven temperature was set to +40 °C. The LC−MS data were acquired using a Waters Synapt G2 quadrupole-time-of-flight (QTOF) high definition mass spectrometer (Waters Corp., Milford, MA, USA) equipped with a LockSpray electrospray ionization source. A positive ionization mode of electrospray was used with a cone voltage of 40 V and a mass range of m/z 100−600. The mass spectrometer and UPLC system were operated using MassLynx 4.1 software. Leucine enkephalin was used as a lock mass compound ($[M + H]^+$: 556.2771).

Plasmids. Rat BNP minimal promoter containing luciferase reporter vector and minimal promoter together with −90 tandem GATA-site have been described previously.[9] The plasmid expressing the mouse GATA4 (pMT2-GATA4) and the empty pMT2 plasmid were gifts from D. B. Wilson (Department of Pediatrics, St. Louis Children's Hospital),[67] and the plasmid expressing the mouse NKX2-5 (pEF-FLAG-NKX2-5) was provided by R. P. Harvey (the Victor Chang Cardiac Research Institute, Darlinghurst, Australia).[68] The mouse NKX2-5 cDNA sequence was cloned from the pEF-plasmid to the pMT2-plasmid as previously described.[15] The p3xNKE-luc plasmid was inserted into the pGL3 basic reporter vector containing a rat albumin minimal promoter with a TATA-box (−40 to +28), which was a kind gift from J. Hakkola (Department of Pharmacology and Toxicology, University of Oulu, Finland)[69] as previously described.[15] The internal control vector pRL-TKd238 was a gift from J. F. Strauss III (University of Pennsylvania School of Medicine, Philadelphia).[70]

In Vitro Screening. In total, 800 small molecules were analyzed in vitro using an immunoprecipitation assay or a luciferase reporter gene assay specifically developed for the GATA4−NKX2-5 transcriptional synergy. For the luciferase reporter assay, mammalian COS-1 cells were cultured on 48-well plates (Greiner Bio One) in Dulbecco's modified Eagle's medium (Sigma-Aldrich/Gibco) containing 10% fetal bovine serum (Gibco) and 1% penicillin−streptomycin (Sigma-Aldrich) (100 U/mL and 0.1 mg/mL, respectively). In addition to co-transfecting all wells with the firefly luciferase reporter vector p3xNKE-luc and the internal control Renilla luciferase vector pRL-TKd238, one set of cells was transfected with the protein expression vector pMT2-GATA4, one set of cells was transfected with pMT2-NKX2-5, one set of cells was transfected with both pMT2-GATA4 and pMT2-NKX2-5, and the final set of cells was transfected with the empty control vector pMT2. For the transfections, the ratio of DNA/transfection reagent (Fugene 6, Roche Applied Science) was 1:3. The total plasmid DNA concentration was normalized across all wells by adding the empty vector pMT2. The compounds were added to the cells 6 h after the transfections, and each well contained 0.1% DMSO. The medium containing the compounds was changed to a fresh one 24 h after the transfection. Thirty hours after the transfection, the cells were lysed with 1× passive lysis buffer (E194A, Promega). The samples were processed on a dual-luciferase assay system (E1960, Promega) according to manufacturer's protocol and measured with a luminometer (Luminoskan RS, Labsystems, Helsinki, Finland). Each compound was tested in two parallel samples. For the analysis of the results, the Firefly values were divided by the Renilla values and then normalized to the vehicle-treated control values.

COS-1 Cell Culture. COS-1 cells were cultured as previously described.[15] For the nuclear protein extractions, the cells were plated in 25 cm^2 cell culture bottles 24 h before the transfection. The pMT2-GATA4 or pMT2-NKX2-5 plasmids were transfected as described above. After 48 h, the transfected cells were collected.

BNP Reporter Assay. COS-1 cells were cultured on 48-well plates (Greiner Bio One) in Dulbecco's modified Eagle's medium (Sigma-Aldrich/Gibco) containing 10% fetal bovine serum (Gibco) and 1% penicillin−streptomycin (Sigma-Aldrich) (100 U/mL and 0.1 mg/mL, respectively). In addition to co-transfecting all wells with the firefly luciferase reporter vector containing either BNP minimal promoter or −90 bp BNP promoter and the internal control Renilla luciferase vector pRL-TKd238, one set of cells was transfected with the protein expression vector pMT2-GATA4 and another set of cells was transfected with the empty vector pMT2. The compounds were added to the cells 6 h after the transfections; each well contained 0.1% DMSO. The medium was changed to a fresh one 24 h after the transfection, and also fresh compounds were added to the cells. Thirty hours after the transfection, the cells were lysed with 1× passive lysis buffer (E194A, Promega). The samples were processed on a dual-luciferase assay system (E1960, Promega) according to the manufacturer's protocol and measured with a luminometer (Luminoskan RS, Labsystems, Helsinki, Finland). Each compound was tested in three parallel samples. For the analysis of the results, the firefly values were divided by the Renilla values and then normalized to the vehicle-treated control values.

Neonatal Cardiomyocyte Culture. The cell culture reagents were obtained from Sigma-Aldrich unless otherwise stated. Primary cultures of neonatal rat ventricular cardiomyocytes were prepared from 2- to 4-day-old Sprague-Dawley or Wistar rats.[14] The animals were sacrificed by decapitation, and the ventricles were excised and cut into small pieces. The ventricle pieces were incubated at 37 °C by shaking for 2 h in a solution containing 100 mM NaCl, 10 mM KCl, 1.2 mM KH_2PO_4, 4.0 mM $MgSO_4$, 50 mM taurine, 20 mM glucose, 10 mM Hepes, 2 mg/mL collagenase type 2 (Worthington, Lakewood), 2 mg/mL pancreatin, and 1% PS (Gibco). After the incubation, the cell suspension was collected into 15 mL tubes and centrifuged for 5 min at 160g. The supernatant and the top layer of the pellet containing the damaged cells were discarded, and the isolated cardiomyocytes were suspended in Dulbecco's modified Eagle medium (DMEM)/F12 culture medium containing 2.5 mM L-glutamine, supplemented with 1% PS and 10% fetal bovine serum (Gibco). The cells were preplated for 30−90 min on cell culture plates with a 10 cm diameter, and the unattached cardiomyocytes were collected with the medium. The number of viable cells was determined, and the cells were seeded onto six-well plates (Corning) at a density of (1.5−2) × 10^5 cells/well according to the assay used. The following day, the medium was replaced with complete serum free medium (CSFM; DMEM/F12, 2.5 mg/mL bovine serum albumin, 1 μM insulin, 2.5 mM L-glutamine, 32 nM selenium, 2.8 mM sodium pyruvate, 5.64 μg/mL transferrin, 1 nM T3, and 100 IU/mL PS). The cells were cultured for another 24 h before adding the compounds. For the DNA binding assay, the cells were treated for 24 h with the compounds at a concentration of 50 μM. For the analysis of the hypertrophic gene expression, the cells were treated with 100 nM endothelin 1 (ET-1, Sigma-Aldrich) for 24 h, and compounds were added to the cells 1 h prior to addition of ET-1. The temperature in the culture chamber was 37 °C with 5% CO_2 and 95% air atmosphere.

Nuclear Protein Extraction. After the appropriate treatments, the cultured cells were washed, and the protein extracts were prepared as previously described.[14,71]

DOI: 10.1021/acs.jmedchem.7b00816
J. Med. Chem. 2017, 60, 7781−7798

Coimmunoprecipitation Assay. GATA4 and NKX2-5 FLAG proteins as well the cell lysate without transfection were produced in COS-1 cells. Agarose bound anti-FLAG M2 antibody (Sigma) was incubated with proteins in lysis buffer (20 mM Tris, 150 mM NaCl, 1 mM EDTA, 1 mM EGTA, 1% Triton X-100, 2.5 mM sodium pyrophosphate) supplemented with protease and phosphatase inhibitors (200 μM sodium orthovanadate, 20 μg/mL leupeptin, 2 μg/mL pepstatin, 20 μg/mL aprotinin, 1 mM phenylmethanesulfonyl fluoride, 50 mM sodium fluoride, 6 μg/mL *N*-tosyl-L-phenylalaninyl-chloromethyl ketone, 6 μg/mL *N*-α-tosyl-L-lysinyl-chloromethyl ketone) overnight at +4 °C with gentle end-over-end mixing. The beads were collected by quick spin with a table top microcentrifuge and washed three times with lysis buffer. The immunoprecipitated proteins were eluted from the agarose beads by boiling the samples in SDS-loading buffer, resolved by SDS−PAGE, transferred onto Optitran BA-S 85 reinforced nitrocellulose membrane (Schleicher & Schuell) and immunoblotted with anti-GATA4 polyclonal antibody (sc-9053, Santa Cruz Biotechnology) and anti-NKX2-5 polyclonal antibody (sc-8697, Santa Cruz Biotechnology). Horseradish peroxidase conjugated anti-rabbit IgG or anti-goat IgG was used as secondary antibody. The immune complex was visualized by using an ECL detection kit (Amersham Pharmacia Biotech) followed by exposure to film (Hyperfilm ECL, Amersham Biosciences) or digitalization of chemiluminescence with luminescent imager analyzer LAS-3000 (Fujifilm). All results were quantitated by using Quantitiy One software (Bio-Rad).

Isolation and Analysis of RNA. Total RNA from the cultured cardiomyocytes was isolated with TRIzol reagent (Invitrogen) following the manufacturer's protocol using the phase lock gel system (Eppendorf AG). For the quantitative real-time polymerase chain reaction (RT-PCR) analyses, cDNA was synthesized from the total RNA using a first-strand cDNA synthesis kit (GE Healthcare Life Sciences) following the manufacturer's protocol. The RNA was analyzed by RT-PCR on an ABI 7300 sequence detection system (Applied Biosystems) using TaqMan chemistry. The sequences of the forward and reverse primers and fluorogenic probes for the RNA detection are shown in Table 5. The results were normalized to 18S RNA quantified from the same samples.

Table 5. Forward and Reverse Primers and Fluorogenic Probe Sequences Used for the Quantitative RT-PCR Analysis

gene		sequence
ANP	forward	GAAAAGCAAACTGAGGGCTCTG
	reverse	CCTACCCCCGAAGCAGCT
	fluorogenic probe	TCGCTGGCCCTCGGAGCCT
BNP	forward	TGGGCAGAAGATAGACCGGA
	reverse	ACAACCTCAGCCCGTCACAG
	fluorogenic probe	CGGCGCAGTCAGTCGCTTGG
18S	forward	TGGTTGCAAAGCTGAAACTTAAAG
	reverse	AGTCAAATTAAGCCGCAGGC
	fluorogenic probe	CCTGGTGGTGCCCTTCCGTCA

Mechanical Stretching of Cardiomyocytes. After the cell isolation, the neonatal rat ventricular cardiomyocytes were seeded at a density of 10^6 cells/well on collagen I coated flexible-bottomed six-well plates (BioFlex collagen I, Flexcell International Corp., Burlington, NC) and cultured for 48 h before the treatments. The cardiomyocytes were exposed to the compounds or vehicle in CSFM and subjected to equibiaxial cyclic mechanical stretching (0.5 Hz, 10−20% elongation) for 48 h using a FlexCell tension system FX-5000 (Flexcell International Corp., Burlington, NC). Nonstretched cardiomyocytes seeded on similar BioFlex plates served as controls.

Immunofluorescence Staining. To investigate the effect of the stretching on the cardiomyocyte size, the cells were washed twice with PBS and fixed with 4% paraformaldehyde for 20 min at room temperature (rt) immediately after the 48 h stretching. The cells were then washed with 0.2% bovine serum albumin in Dulbecco's PBS (DB) and permeabilized with 0.1% Triton X-100 in PBS for 10 min at rt, followed by two 10 min washes in DB. Square pieces (10−15 mm × 10−15 mm) of the silicone membranes were then cut from the centers of the wells, incubated with a primary antibody against sarcomeric α-actinin (at 1:800 in DB, Sigma-Aldrich A7811) for 60 min at rt, washed three times for 10 min with DB, and incubated with the Alexa Fluor 488 anti-mouse secondary antibody (at 1:200 in DB, Life Technologies A-11029) and Alexa Fluor 647 phalloidin (at 1:140 in DB, Life Technologies A22287) for 45 min at rt. After three 10 min washes with DB, the specimens were mounted on microscopy slides using ProLong Gold Antifade Mountant with DAPI (Molecular Probes) and cured overnight at RT, after which they were stored at 4−8 °C.

Analysis of the Cell Surface Area. For the cell surface area analysis, a minimum of six images of each stretched or nonstretched specimen were captured with a Hamamatsu Orca-Flash4.0 V2 camera (Hamamatsu Photonics, Hamamatsu, Japan) attached to a Leica DM6000B fluorescence microscope using 20×/0.7 HC PL APO CS2 objective and Leica Application Suite X software (Leica Microsystems, Wetzlar, Germany). The cell surface areas of the cardiomyocytes were determined from the images using CellProfiler software.[72,73] In brief, the nuclei were identified based on DAPI staining, followed by the detection of cell edges using an overlay of the fluorescence images of α-actinin and phalloidin. The cells were then filtered based on the α-actinin staining, and the surface areas of the α-actinin$^+$ cells (cardiomyocytes) were determined. The mean cell surface areas were calculated for each specimen (>200 cells/specimen) and normalized to the mean cell surface area of the untreated, nonstretched cardiomyocytes from the same experiment.

DNA Binding Properties. The effect of the compounds on the DNA binding abilities of GATA4 and NKX2-5 was studied by performing an electrophoretic mobility shift assay (EMSA). The GATA4 or NKX2-5 proteins used in the binding reactions were overexpressed proteins from the COS-1 cells or endogenous proteins from neonatal rat cardiomyocytes treated with the compounds for 24 h before the nuclear protein extraction. The nuclear protein extracts from the cells were incubated with a radioactively labeled double stranded oligonucleotide, which contained either the GATA4 or NKX2-5 specific binding site. For GATA4, the double-stranded oligonucleotide corresponded to the GATA binding region −90, i.e., Δ−68/−97 of the rat BNP promoter (GenBank code M60266) as follows: rBNP −90 tandem GATA (5′-TGTGTCTGATAAAT-CAGAGATAACCCCACC-3′). For NKX2-5, the double-stranded oligonucleotide corresponded to the NKX2-5 binding element in the ANP promoter region (GenBank code M27498) as follows: rANP −240 NKE-like element (5′-AGAGACCTTTGAAGTGGGGGCC-TCTTGAGGCCCCG-3′). The probes were sticky-end-labeled with [α-^{32}P]dCTP by Klenow enzyme. For each binding reaction mixture, the nuclear/total GATA4 or NKX2-5 protein was used in a final concentration of 16 mM HEPES, 120 mM NaCl, 0.67 mM EDTA, 0.3 mM EGTA, 8% glycerol, 0.02% NP-40, 40 mM KCl, 1 mM $MgCl_2$, 0.1 μg/μL poly(dIxdC)$_2$, 0.5 mM Tris-HCl (pH 7.5), 1 mM PMSF, 40 μg/mL aprotinin, 40 μg/mL leupeptin, and 4 μg/mL pepstatin. The final volume of the binding reaction was equalized to 20 μL with a high salt buffer. Reaction mixtures containing the nuclear proteins from the COS-1 cells were incubated with the compounds for 10 min before adding the labeled probes. After 20 min of incubating the nuclear protein with the probe, the protein−DNA mixtures were separated by nondenaturating gel electrophoresis on 5% polyacrylamide gel. For the supershift assay, either the GATA4 antibody (sc-1237X, Santa Cruz Biotechnology) or NKX2-5 antibody (sc-8697X, Santa Cruz Biotechnology) was incubated for 10 min with the protein sample before adding the compounds. Subsequently, the gels were dried and exposed to PhosphorImager screens (Molecular Dynamics, Sunnyvale, CA, USA). The screens were scanned using a Bio-Rad molecular imager FX Pro Plus and analyzed with Quantity One software (Bio-Rad Laboratories).

In Vitro Cytotoxicity. The release of adenylate kinase (AK) from the ruptured rat cardiac cells into the cell culture medium was analyzed

DOI: 10.1021/acs.jmedchem.7b00816
J. Med. Chem. 2017, 60, 7781−7798

using a ToxiLight bioassay kit (nondestructive cytotoxicity assay) from Lonza Rockland Inc. (Rockland, ME, USA) according to the manufacturer's instructions. A luminometer (Luminoskan RS, Labsystems, Helsinki, Finland) was used to measure the bioluminescence of AK in the medium after 24 h of treatment with the compounds at a concentration of 50 μM. To detect the apoptotic myocytes, a terminal deoxynucleotidyl transferase-mediated dUTP nick end-labeling (TUNEL) assay was performed. The rat cardiac myocytes were plated onto Nunc Lab-Tek chamber slide system eight-well slides (Thermo Fisher Scientific Inc.). The cells were treated with the compounds at a concentration of 50 μM for 24 h. The apoptotic cells were detected using the ApopTag peroxidase in situ apoptosis detection kit (Millipore).

In Vitro Kinase Profiling. The effect of the compounds **3** and **4** on the activity of 48 kinases was assessed by Cerep's ExpresS Diversity kinase profile service (Cerep, France). The compounds were tested at a concentration 30 μM in duplicate.

GPCR Profiling. The effect of the compound **3** in terms of GPCR agonism and antagonism was tested by GPCRProfiler (Millipore, Germany), which comprises cell-based functional assays for 165 GPCRs. The compound was used to test agonistic activities at a concentration of 12.5 μM and antagonistic activities at a concentration of 10 μM in duplicate.

Statistics. The results are expressed as the mean ± standard deviation (SD). The statistical analyses were performed using SPSS version 22 (SPSS Inc., Chicago, IL, USA). To determine the significant difference between two groups, independent samples of Student's *t*-tests were used. For multiple comparisons, the statistical significance was evaluated by one-way analysis of variance (ANOVA), followed by Bonferroni post hoc tests. The probability values of (*) $p < 0.05$, (**) $p < 0.01$, and (***) $p < 0.001$ were considered statistically significant.

■ ASSOCIATED CONTENT

Supporting Information

The Supporting Information is available free of charge on the ACS Publications website at DOI: 10.1021/acs.jmedchem.7b00816.

Additional figures and tables illustrating compounds aggregation, chemical stability, effects on GATA4 transcriptional activity, the protein kinases and the GPCRs, coimmunoprecipitation assay results, and the original EMSA gel samples (PDF)

Coordinates information for structure representation (PDB)

Molecular formula strings and some data (CSV)

■ AUTHOR INFORMATION

Corresponding Author

*Phone: +358-50-4480722, E-mail: heikki.ruskoaho@helsinki.fi.

ORCID

Mika J. Välimäki: 0000-0002-9687-8197

Author Contributions

‖M.J.V. and M.A.T. contributed equally to the work and are considered co-first-authors. H.J.R, M.J.V, M.A.T, S.M.K, and A.P. conceived and designed the experiments. M.J.V, M.A.T, S.M.K, J.A., R.S., L.P, and V.T. performed the experiments. M.J.V, M.A.T, S.M.K., J.A., R.S., H.J.R., A.P., L.P., and V.T. analyzed the data. The manuscript was written with contributions from all authors. All authors have approved the final version of the manuscript.

Notes

The authors declare no competing financial interest.

The authors will release the atomic coordinates and experimental data upon article publication.

■ ACKNOWLEDGMENTS

We thank Marja Arbelius, Kirsi Salo, Nina Sipari, Niklas Johansson, and Gustav Boije af Gennäs for their expert technical assistance. This work was supported by the Finnish Funding Agency for Innovation (Tekes, 3iRegeneration, Project 40395/13), the Academy of Finland (Project 2666621), the Finnish Foundation for Cardiovascular Research, and the Sigrid Jusélius Foundation.

■ ABBREVIATIONS USED

AK, adenylate kinase; ANP, atrial natriuretic peptide; BNP, B-type natriuretic peptide; DMEM, Dulbecco's modified Eagle's medium; FBS, fetal bovine serum; FGFR3, fibroblast growth factor receptor 3 kinase; FOG, Friend of GATA; EBDM, embryoid body differentiation medium; EMSA, electrophoretic mobility shift assay; ET-1, endothelin-1; HEPES, 4-(2-hydroxyethyl)-1-piperazineethanesulfonic acid; K_a, synergy activation; KDR, kinase insert domain receptor; MEF2, myocyte-specific enhancer factor 2; mESC, mouse embryonic stem cell; MHC, myosin heavy chain; NKE, NKX2-5 high affinity response element; PMSF, phenylmethanesulfonyl fluoride; PS, penicillin−streptomycin; PTM, post-translational modification; QTOF, quadrupole-time-of-flight; ROCK1, Rho-associated protein kinase 1; SRE, serum response element; SRF, serum response factor; TBTU, *O*-(benzotriazol-1-yl)-*N*,*N*,*N*′,*N*′-tetramethyluronium tetrafluoroborate; TF, transcription factor; TUNEL, terminal deoxynucleotidyl transferase dUTP nick end-labeling; UPLC, ultraperformance liquid chromatography

■ REFERENCES

(1) Levine, M.; Tjian, R. Transcription Regulation and Animal Diversity. *Nature* **2003**, *424*, 147−151.

(2) Spitz, F.; Furlong, E. E. Transcription Factors: From Enhancer Binding to Developmental Control. *Nat. Rev. Genet.* **2012**, *13*, 613−626.

(3) Flores, N. M.; Oviedo, N. J.; Sage, J. Essential Role for the Planarian Intestinal GATA Transcription Factor in Stem Cells and Regeneration. *Dev. Biol.* **2016**, *418*, 179−188.

(4) Molkentin, J. D.; Lin, Q.; Duncan, S. A.; Olson, E. N. Requirement of the Transcription Factor GATA4 for Heart Tube Formation and Ventral Morphogenesis. *Genes Dev.* **1997**, *11*, 1061−1072.

(5) Lyons, I.; Parsons, L. M.; Hartley, L.; Li, R.; Andrews, J. E.; Robb, L.; Harvey, R. P. Myogenic and Morphogenetic Defects in the Heart Tubes of Murine Embryos Lacking the Homeo Box Gene Nkx2-5. *Genes Dev.* **1995**, *9*, 1654−1666.

(6) Horb, M. E.; Thomsen, G. H. Tbx5 Is Essential for Heart Development. *Development* **1999**, *126*, 1739−1751.

(7) Grepin, C.; Nemer, G.; Nemer, M. Enhanced Cardiogenesis in Embryonic Stem Cells Overexpressing the GATA-4 Transcription Factor. *Development* **1997**, *124*, 2387−2395.

(8) Mercola, M.; Ruiz-Lozano, P.; Schneider, M. D. Cardiac Muscle Regeneration: Lessons from Development. *Genes Dev.* **2011**, *25*, 299−309.

(9) Grepin, C.; Dagnino, L.; Robitaille, L.; Haberstroh, L.; Antakly, T.; Nemer, M. A Hormone-Encoding Gene Identifies a Pathway for Cardiac but Not Skeletal Muscle Gene Transcription. *Mol. Cell. Biol.* **1994**, *14*, 3115−3129.

(10) Thuerauf, D. J.; Hanford, D. S.; Glembotski, C. C. Regulation of Rat Brain Natriuretic Peptide Transcription. A Potential Role for

DOI: 10.1021/acs.jmedchem.7b00816
J. Med. Chem. 2017, 60, 7781−7798

GATA-Related Transcription Factors in Myocardial Cell Gene Expression. *J. Biol. Chem.* **1994**, *269*, 17772−17775.
(11) Molkentin, J. D.; Kalvakolanu, D. V.; Markham, B. E. Transcription Factor GATA-4 Regulates Cardiac Muscle-Specific Expression of the Alpha-Myosin Heavy-Chain Gene. *Mol. Cell. Biol.* **1994**, *14*, 4947−4957.
(12) Hasegawa, K.; Lee, S. J.; Jobe, S. M.; Markham, B. E.; Kitsis, R. N. Cis-Acting Sequences That Mediate Induction of Beta-Myosin Heavy Chain Gene Expression during Left Ventricular Hypertrophy due to Aortic Constriction. *Circulation* **1997**, *96*, 3943−3953.
(13) Pikkarainen, S.; Tokola, H.; Kerkela, R.; Ruskoaho, H. GATA Transcription Factors in the Developing and Adult Heart. *Cardiovasc. Res.* **2004**, *63*, 196−207.
(14) Pikkarainen, S.; Tokola, H.; Majalahti-Palviainen, T.; Kerkela, R.; Hautala, N.; Bhalla, S. S.; Charron, F.; Nemer, M.; Vuolteenaho, O.; Ruskoaho, H. GATA-4 Is a Nuclear Mediator of Mechanical Stretch-Activated Hypertrophic Program. *J. Biol. Chem.* **2003**, *278*, 23807−23816.
(15) Kinnunen, S.; Välimäki, M.; Tölli, M.; Wohlfahrt, G.; Darwich, R.; Komati, H.; Nemer, M.; Ruskoaho, H. Nuclear Receptor-like Structure and Interaction of Congenital Heart Disease-Associated Factors GATA4 and NKX2-5. *PLoS One* **2015**, *10*, e0144145.
(16) Schlesinger, J.; Schueler, M.; Grunert, M.; Fischer, J. J.; Zhang, Q.; Krueger, T.; Lange, M.; Tönjes, M.; Dunkel, I.; Sperling, S. R. The Cardiac Transcription Network Modulated by Gata4, Mef2a, Nkx2.5, Srf, Histone Modifications, and microRNAs. *PLoS Genet.* **2011**, *7*, e1001313.
(17) Charron, F.; Tsimiklis, G.; Arcand, M.; Robitaille, L.; Liang, Q.; Molkentin, J. D.; Meloche, S.; Nemer, M. Tissue-Specific GATA Factors Are Transcriptional Effectors of the Small GTPase RhoA. *Genes Dev.* **2001**, *15*, 2702−2719.
(18) Yanazume, T.; Hasegawa, K.; Morimoto, T.; Kawamura, T.; Wada, H.; Matsumori, A.; Kawase, Y.; Hirai, M.; Kita, T. Cardiac p300 Is Involved in Myocyte Growth with Decompensated Heart Failure. *Mol. Cell. Biol.* **2003**, *23*, 3593−3606.
(19) Wang, J.; Feng, X. H.; Schwartz, R. J. SUMO-1 Modification Activated GATA4-Dependent Cardiogenic Gene Activity. *J. Biol. Chem.* **2004**, *279*, 49091−49098.
(20) Ieda, M.; Fu, J. D.; Delgado-Olguin, P.; Vedantham, V.; Hayashi, Y.; Bruneau, B. G.; Srivastava, D. Direct Reprogramming of Fibroblasts into Functional Cardiomyocytes by Defined Factors. *Cell* **2010**, *142*, 375−386.
(21) Song, K.; Nam, Y. J.; Luo, X.; Qi, X.; Tan, W.; Huang, G. N.; Acharya, A.; Smith, C. L.; Tallquist, M. D.; Neilson, E. G.; Hill, J. A.; Bassel-Duby, R.; Olson, E. N. Heart Repair by Reprogramming Non-Myocytes with Cardiac Transcription Factors. *Nature* **2012**, *485*, 599−604.
(22) Kang, C.; Xu, Q.; Martin, T. D.; Li, M. Z.; Demaria, M.; Aron, L.; Lu, T.; Yankner, B. A.; Campisi, J.; Elledge, S. J. The DNA Damage Response Induces Inflammation and Senescence by Inhibiting Autophagy of GATA4. *Science* **2015**, *349*, aaa5612.
(23) El-Hachem, N.; Nemer, G. Identification of New GATA4-Small Molecule Inhibitors by Structure-Based Virtual Screening. *Bioorg. Med. Chem.* **2011**, *19*, 1734−1742.
(24) Durocher, D.; Nemer, M. Combinatorial Interactions Regulating Cardiac Transcription. *Dev. Genet.* **1998**, *22*, 250−262.
(25) Sepulveda, J. L.; Belaguli, N.; Nigam, V.; Chen, C. Y.; Nemer, M.; Schwartz, R. J. GATA-4 and Nkx-2.5 Coactivate Nkx-2 DNA Binding Targets: Role for Regulating Early Cardiac Gene Expression. *Mol. Cell. Biol.* **1998**, *18*, 3405−3415.
(26) Auld, D. S.; Inglese, J. Interferences with Luciferase Reporter Enzymes. In *Assay Guidance Manual*; Sittampalam, G., Coussens, N., Brimacombe, K., Grossman, A., Arkin, M., Auld, D., Austin, C., Baell, J., Bejcek, B., Chung, T., Dahlin, J., Devanaryan, V., Foley, T., Glicksman, M., Hall, M., Hass, J., Inglese, J., Iversen, P., Kahl, S., Kales, S., Lal-Nag, M., Li, Z., McGee, J., McManus, O., Xu, X., Eds.; Eli Lilly & Company and the National Center for Advancing Translational Sciences: Bethesda, MD, 2016; Vol. *1*, pp 1−14, http://www.ncbi.nlm.nih.gov/books/NBK374281/ (accessed August 10, 2017).
(27) Miranker, A.; Karplus, M. Functionality Maps of Binding Sites: A Multiple Copy Simultaneous Search Method. *Proteins: Struct., Funct., Genet.* **1991**, *11*, 29−34.
(28) Kinnunen, S.; Tölli, M.; Välimäki, M.; Jumppanen, M.; Boije af Gennäs, G.; Yli-Kauhaluoma, J.; Ruskoaho, H. Pharmaceutical Compounds. Patent Application 20165712, 2016.
(29) Lee, Y.; Shioi, T.; Kasahara, H.; Jobe, S. M.; Wiese, R. J.; Markham, B. E.; Izumo, S. The Cardiac Tissue-Restricted Homeobox Protein Csx/Nkx2.5 Physically Associates with the Zinc Finger Protein GATA4 and Cooperatively Activates Atrial Natriuretic Factor Gene Expression. *Mol. Cell. Biol.* **1998**, *18*, 3120−3129.
(30) Durocher, D.; Charron, F.; Warren, R.; Schwartz, R. J.; Nemer, M. The Cardiac Transcription Factors Nkx2-5 and GATA-4 Are Mutual Cofactors. *EMBO J.* **1997**, *16*, 5687−5696.
(31) Kinnunen, P.; Vuolteenaho, O.; Uusimaa, P.; Ruskoaho, H. Passive Mechanical Stretch Releases Atrial Natriuretic Peptide from Rat Ventricular Myocardium. *Circ. Res.* **1992**, *70*, 1244−1253.
(32) LaPointe, M. C. Molecular Regulation of the Brain Natriuretic Peptide Gene. *Peptides* **2005**, *26*, 944−956.
(33) Nakagawa, O.; Ogawa, Y.; Itoh, H.; Suga, S.; Komatsu, Y.; Kishimoto, I.; Nishino, K.; Yoshimasa, T.; Nakao, K. Rapid Transcriptional Activation and Early mRNA Turnover of Brain Natriuretic Peptide in Cardiocyte Hypertrophy. Evidence for Brain Natriuretic Peptide as an "Emergency" Cardiac Hormone against Ventricular Overload. *J. Clin. Invest.* **1995**, *96*, 1280−1287.
(34) Xin, Z.; Zhao, H.; Serby, M. D.; Liu, B.; Schaefer, V. G.; Falls, D. H.; Kaszubska, W.; Colins, C. A.; Sham, H. L.; Liu, G. Synthesis and Structure−activity Relationships of Isoxazole Carboxamides as Growth Hormone Secretagogue Receptor Antagonists. *Bioorg. Med. Chem. Lett.* **2005**, *15*, 1201−1204.
(35) Omichinski, J. G.; Clore, G. M.; Schaad, O.; Felsenfeld, G.; Trainor, C.; Appella, E.; Stahl, S. J.; Gronenborn, A. M. NMR Structure of a Specific DNA Complex of Zn-Containing DNA Binding Domain of GATA-1. *Science* **1993**, *261*, 438−446.
(36) Katanasaka, Y.; Suzuki, H.; Sunagawa, Y.; Hasegawa, K.; Morimoto, T. Regulation of Cardiac Transcription Factor GATA4 by Post-Translational Modification in Cardiomyocyte Hypertrophy and Heart Failure. *Int. Heart J.* **2016**, *57*, 672−675.
(37) Lee, T. I.; Young, R. A. Transcriptional Regulation and Its Misregulation in Disease. *Cell* **2013**, *152*, 1237−1251.
(38) Hagenbuchner, J.; Ausserlechner, M. J. Targeting Transcription Factors by Small Compounds–Current Strategies and Future Implications. *Biochem. Pharmacol.* **2016**, *107*, 1−13.
(39) Addis, R. C.; Ifkovits, J. L.; Pinto, F.; Kellam, L. D.; Esteso, P.; Rentschler, S.; Christoforou, N.; Epstein, J. A.; Gearhart, J. D. Optimization of Direct Fibroblast Reprogramming to Cardiomyocytes Using Calcium Activity as a Functional Measure of Success. *J. Mol. Cell. Cardiol.* **2013**, *60*, 97−106.
(40) Srivastava, D.; Ieda, M. Critical Factors for Cardiac Reprogramming. *Circ. Res.* **2012**, *111*, 5−8.
(41) Xin, M.; Olson, E. N.; Bassel-Duby, R. Mending Broken Hearts: Cardiac Development as a Basis for Adult Heart Regeneration and Repair. *Nat. Rev. Mol. Cell Biol.* **2013**, *14*, 529−541.
(42) Morin, S.; Charron, F.; Robitaille, L.; Nemer, M. GATA-Dependent Recruitment of MEF2 Proteins to Target Promoters. *EMBO J.* **2000**, *19*, 2046−2055.
(43) Dai, Y. S.; Cserjesi, P.; Markham, B. E.; Molkentin, J. D. The Transcription Factors GATA4 and dHAND Physically Interact to Synergistically Activate Cardiac Gene Expression through a p300-Dependent Mechanism. *J. Biol. Chem.* **2002**, *277*, 24390−24398.
(44) Garg, V.; Kathiriya, I. S.; Barnes, R.; Schluterman, M. K.; King, I. N.; Butler, C. A.; Rothrock, C. R.; Eapen, R. S.; Hirayama-Yamada, K.; Joo, K.; Matsuoka, R.; Cohen, J. C.; Srivastava, D. GATA4 Mutations Cause Human Congenital Heart Defects and Reveal an Interaction with TBX5. *Nature* **2003**, *424*, 443−447.
(45) Ang, Y.-S.; Rivas, R. N.; Ribeiro, A. J. S.; Srivas, R.; Rivera, J.; Stone, N. R.; Pratt, K.; Mohamed, T. M. A.; Fu, J.-D.; Spencer, C. I.; Tippens, N. D.; Li, M.; Narasimha, A.; Radzinsky, E.; Moon-Grady, A. J.; Yu, H.; Pruitt, B. L.; Snyder, M. P.; Srivastava, D. Disease Model of

DOI: 10.1021/acs.jmedchem.7b00816
J. Med. Chem. 2017, 60, 7781−7798

GATA4 Mutation Reveals Transcription Factor Cooperativity in Human Cardiogenesis. *Cell* **2016**, *167*, 1734−1749.
(46) Belaguli, N. S.; Sepulveda, J. L.; Nigam, V.; Charron, F.; Nemer, M.; Schwartz, R. J. Cardiac Tissue Enriched Factors Serum Response Factor and GATA-4 Are Mutual Coregulators. *Mol. Cell. Biol.* **2000**, *20*, 7550−7558.
(47) Nam, Y. J.; Song, K.; Olson, E. N. Cardiac Repair by Reprogramming of Cardiac Fibroblasts into Cardiomyocytes. Patent WO2012/116064 A1, 2012.
(48) Schorpp, K.; Rothenaigner, I.; Salmina, E.; Reinshagen, J.; Low, T.; Brenke, J. K.; Gopalakrishnan, J.; Tetko, I. V.; Gul, S.; Hadian, K. Identification of Small-Molecule Frequent Hitters from AlphaScreen High-Throughput Screens. *J. Biomol. Screening* **2014**, *19*, 715−726.
(49) Tomašić, T.; Peterlin Mašič, L. Rhodanine as a Scaffold in Drug Discovery: A Critical Review of Its Biological Activities and Mechanisms of Target Modulation. *Expert Opin. Drug Discovery* **2012**, *7*, 549−560.
(50) Schade, D.; Plowright, A. T. Medicinal Chemistry Approaches to Heart Regeneration. *J. Med. Chem.* **2015**, *58*, 9451−9479.
(51) Davies, S. G.; Kennewell, P. D.; Russell, A. J.; Seden, P. T.; Westwood, R.; Wynne, G. M. Stemistry: The Control of Stem Cells in Situ Using Chemistry. *J. Med. Chem.* **2015**, *58*, 2863−2894.
(52) Kimelman, D. Mesoderm Induction: From Caps to Chips. *Nat. Rev. Genet.* **2006**, *7*, 360−372.
(53) Witty, A. D.; Mihic, A.; Tam, R. Y.; Fisher, S. A.; Mikryukov, A.; Shoichet, M. S.; Li, R. K.; Kattman, S. J.; Keller, G. Generation of the Epicardial Lineage from Human Pluripotent Stem Cells. *Nat. Biotechnol.* **2014**, *32*, 1026−1035.
(54) Cao, N.; Huang, Y.; Zheng, J.; Spencer, C. I.; Zhang, Y.; Fu, J.-D.; Nie, B.; Xie, M.; Zhang, M.; Wang, H.; Ma, T.; Xu, T.; Shi, G.; Srivastava, D.; Ding, S. Conversion of Human Fibroblasts into Functional Cardiomyocytes by Small Molecules. *Science* **2016**, *352*, 1216−1220.
(55) Mohamed, T. M. A.; Stone, N. R.; Berry, E. C.; Radzinsky, E.; Huang, Y.; Pratt, K.; Ang, Y. S.; Yu, P.; Wang, H.; Tang, S.; Magnitsky, S.; Ding, S.; Ivey, K. N.; Srivastava, D. Chemical Enhancement of In Vitro and In Vivo Direct Cardiac Reprogramming. *Circulation* **2017**, *135*, 978−995.
(56) Sadek, H.; Hannack, B.; Choe, E.; Wang, J.; Latif, S.; Garry, M. G.; Garry, D. J.; Longgood, J.; Frantz, D. E.; Olson, E. N.; Hsieh, J.; Schneider, J. W. Cardiogenic Small Molecules That Enhance Myocardial Repair by Stem Cells. *Proc. Natl. Acad. Sci. U. S. A.* **2008**, *105*, 6063−6068.
(57) Russell, J. L.; Goetsch, S. C.; Aguilar, H. R.; Coe, H.; Luo, X.; Liu, N.; van Rooij, E.; Frantz, D. E.; Schneider, J. W. Regulated Expression of pH Sensing G Protein-Coupled Receptor-68 Identified through Chemical Biology Defines a New Drug Target for Ischemic Heart Disease. *ACS Chem. Biol.* **2012**, *7*, 1077−1083.
(58) Ahuja, P.; Sdek, P.; MacLellan, W. R. Cardiac Myocyte Cell Cycle Control in Development, Disease, and Regeneration. *Physiol. Rev.* **2007**, *87*, 521−544.
(59) Addis, R. C.; Epstein, J. A. Induced Regeneration–the Progress and Promise of Direct Reprogramming for Heart Repair. *Nat. Med.* **2013**, *19*, 829−836.
(60) Muraoka, N.; Ieda, M. Direct Reprogramming of Fibroblasts into Myocytes to Reverse Fibrosis. *Annu. Rev. Physiol.* **2014**, *76*, 21−37.
(61) Ma, H.; Wang, L.; Liu, J.; Qian, L. Direct Cardiac Reprogramming as a Novel Therapeutic Strategy for Treatment of Myocardial Infarction. *Methods Mol. Biol.* **2017**, *1521*, 69−88.
(62) Lian, X.; Hsiao, C.; Wilson, G.; Zhu, K.; Hazeltine, L. B.; Azarin, S. M.; Raval, K. K.; Zhang, J.; Kamp, T. J.; Palecek, S. P. Robust Cardiomyocyte Differentiation from Human Pluripotent Stem Cells via Temporal Modulation of Canonical Wnt Signaling. *Proc. Natl. Acad. Sci. U. S. A.* **2012**, *109*, 1848−1857.
(63) Lian, X.; Zhang, J.; Azarin, S. M.; Zhu, K.; Hazeltine, L. B.; Bao, X.; Hsiao, C.; Kamp, T. J.; Palecek, S. P. Directed Cardiomyocyte Differentiation from Human Pluripotent Stem Cells by Modulating Wnt/β-Catenin Signaling under Fully Defined Conditions. *Nat. Protoc.* **2013**, *8*, 162−175.
(64) Labute, P. The Generalized Born/volume Integral Implicit Solvent Model: Estimation of the Free Energy of Hydration Using London Dispersion instead of Atomic Surface Area. *J. Comput. Chem.* **2008**, *29*, 1693−1698.
(65) Lovell, S. C.; Davis, I. W.; Arendall, W. B.; de Bakker, P. I.; Word, J. M.; Prisant, M. G.; Richardson, J. S.; Richardson, D. C. Structure Validation by Calpha Geometry: Phi, Psi and Cbeta Deviation. *Proteins: Struct., Funct., Genet.* **2003**, *50*, 437−450.
(66) Chan, S. L.; Labute, P. Training a Scoring Function for the Alignment of Small Molecules. *J. Chem. Inf. Model.* **2010**, *50*, 1724−1735.
(67) Arceci, R. J.; King, A. A.; Simon, M. C.; Orkin, S. H.; Wilson, D. B. Mouse GATA-4: A Retinoic Acid-Inducible GATA-Binding Transcription Factor Expressed in Endodermally Derived Tissues and Heart. *Mol. Cell. Biol.* **1993**, *13*, 2235−2246.
(68) Ranganayakulu, G.; Elliott, D. A.; Harvey, R. P.; Olson, E. N. Divergent Roles for NK-2 Class Homeobox Genes in Cardiogenesis in Flies and Mice. *Development* **1998**, *125*, 3037−3048.
(69) Hakkola, J.; Hu, Y.; Ingelman-Sundberg, M. Mechanisms of Down-Regulation of CYP2E1 Expression by Inflammatory Cytokines in Rat Hepatoma Cells. *J. Pharmacol. Exp. Ther.* **2003**, *304*, 1048−1054.
(70) Ho, C. K. M.; Strauss, J. F. Activation of the Control Reporter Plasmids pRL-TK and pRL-SV40 by Multiple GATA Transcription Factors Can Lead to Aberrant Normalization of Transfection Efficiency. *BMC Biotechnol.* **2004**, *4*, 10.
(71) Kerkela, R.; Pikkarainen, S.; Majalahti-Palviainen, T.; Tokola, H.; Ruskoaho, H. Distinct Roles of Mitogen-Activated Protein Kinase Pathways in GATA-4 Transcription Factor-Mediated Regulation of B-Type Natriuretic Peptide Gene. *J. Biol. Chem.* **2002**, *277*, 13752−13760.
(72) Carpenter, A. E.; Jones, T. R.; Lamprecht, M. R.; Clarke, C.; Kang, I. H.; Friman, O.; Guertin, D. A.; Chang, J. H.; Lindquist, R. A.; Moffat, J.; Golland, P.; Sabatini, D. M. CellProfiler: Image Analysis Software for Identifying and Quantifying Cell Phenotypes. *Genome Biol.* **2006**, *7*, R100.
(73) Kamentsky, L.; Jones, T. R.; Fraser, A.; Bray, M.-A.; Logan, D. J.; Madden, K. L.; Ljosa, V.; Rueden, C.; Eliceiri, K. W.; Carpenter, A. E. Improved Structure, Function and Compatibility for CellProfiler: Modular High-Throughput Image Analysis Software. *Bioinformatics* **2011**, *27*, 1179−1180.

DOI: 10.1021/acs.jmedchem.7b00816
J. Med. Chem. 2017, 60, 7781−7798